DISULFIDE BOND DETERMINATION BY COMBINING EFFICIENT SEARCH AND MACHINE LEARNING

A thesis submitted to the faculty of
San Francisco State University
In partial fulfillment of
The Requirements for
The Degree

Master of Science
In
Computer Science: Computing for Life Sciences

by
William Henrique Elias Murad

San Francisco State University
December, 2010

CERTIFICATION OF APPROVAL

I certify that I have read *Disulfide Bond Determination by Combining Efficient Search and Machine Learning* by William Henrique Elias Murad, and that in my opinion this work meets the criteria for approving a thesis submitted in partial fulfillment of the requirements for the degree: Master of Science in Computer Science: Computing for Life Sciences at San Francisco State University.

_____

Rahul Singh
Professor of Bioinformatics

_____

Hui Yang
Professor of Data Mining

_____

Robert Yen
Professor of Biochemistry

DISULFIDE BOND DETERMINATION BY COMBINING EFFICIENT SEARCH AND MACHINE LEARNING

William Henrique Elias Murad
San Francisco, California
2010

Background

Determining the disulfide (S-S) bond pattern in a protein is often crucial for understanding its structure and function. In recent research, mass spectrometry (MS) based analysis has been applied to this problem following protein digestion under both partial reduction and non-reduction conditions. However, this paradigm still awaits solutions to certain algorithmic problems fundamental amongst which is the efficient matching of an exponentially growing set of putative S-S bonded structural alternatives to the large amounts of experimental spectrometric data. Current methods circumvent this challenge primarily through simplifications, such as by assuming only the occurrence of certain ion-types (*b*-ions and *y*-ions) that predominate in the more popular dissociation methods, such as collision-induced dissociation (*CID*). Unfortunately, this can adversely impact the quality of results.

Method

This work presents an algorithmic approach to this problem that can, with high computational efficiency, analyze multiple ions types (a, b, b^o, b^*, c, x, y, y^o, y^*, and z) and deal with complex bonding topologies. The proposed approach combines (1) an

approximation algorithm-based search formulation with data driven parameter estimation and (2) machine learning techniques which are used to train a SVM classifier, based on previously annotated data from the Swiss-Prot knowledgebase. This proposed formulation considers only those regions of the search space where the correct solution resides with a high likelihood. Putative disulfide bonds thus obtained are finally combined in a globally consistent pattern to yield the overall disulfide bonding topology of the molecule. Additionally, each bond is associated with either a confidence score (MS-based bonds) or a similarity score (SVM-based bonds), which aid in interpretation and assimilation of the results.

Results

The method was tested on nine different eukaryotic Glycosyltransferases possessing disulfide bonding topologies of varying complexity. Its performance was found to be characterized by high efficiency (in terms of time and the fraction of search space considered), sensitivity, specificity, and accuracy. An implementation of the method is available at: http://tintin.sfsu.edu/~whemurad/disulfidebond.

Conclusions

This work addresses some of the significant challenges in MS-based disulfide bond determination. This is the first algorithmic work that can consider multiple ion types in this problem setting while simultaneously ensuring polynomial time complexity and high accuracy of results. It is also the first solution to combine MS-based methods with machine learning to determine the disulfide linkage of proteins. In this scenario, machine learning techniques are used to circumvent some of the limitations of MS-based methods. The analysis of the results shows that the blend of both state-of-the-art strategies allowed

the implementation of a solution which performed as well or better than the competing techniques.

I certify that the Abstract is a correct representation of the content of this thesis.

_____ _____

Rahul Singh, Chair, Thesis Committee Date

TABLE OF CONTENTS

LIST OF TABLES

Table Page

LIST OF FIGURES

Figure Page

LIST OF APPENDICES

Appendix Page

Introduction

A disulfide bond, also called S-S bond or disulfide bridge, is a single covalent bond formed from the oxidation of sulfhydryl groups (Figure 1). The oxidation process that forms interchain disulfide bonds can produce stable covalently linked proteins, whereas intrachain S-S bonds contribute to folding and stability. Disulfide bonds have been classified into three categories: structural, catalytic or allosteric. Structural disulfide bonds play an important role in the folding and stabilization of proteins. Catalytic bonds mediate thiol-disulfide interchange reactions in substrate proteins and are important for regulation of enzymatic activity. Allosteric disulfide bonds, in contrast to catalytic disulfides, control the functioning of proteins by triggering changes in the intra-molecular or inter-molecular protein structure, acting essentially as switches for protein function [1].

Figure 1 – Disulfide bond formation (left) and cysteine structure (right)

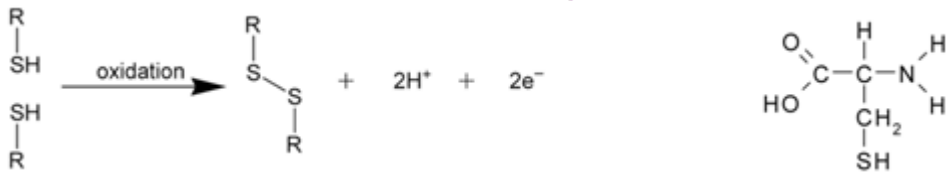

Among the 20 natural amino acids, cysteine is unique because it is involved in many biological activities through oxidation and reduction to form disulfide bonds and sulfhydryls [2]. Disulfide bonds play an important role in understanding protein folding,

evolution, and structural properties, imposing length and angle constraints on the backbone of a protein. Therefore, the identification of proteins disulfide connectivity is crucial to understand their structure and function. However, the determination of disulfide bonds can be a challenging task.

Early computational approaches for S-S bond determination focused on two learning-driven formulations based on the protein primary structure [1]: *residue classification* (distinguish bonded and free cysteines) and *connectivity prediction* (determine the S-S connectivity pattern). In recent times, the increasing availability and accuracy of mass spectrometry [2] (MS) has opened up an alternate approach; its essence lies in matching the theoretical spectra of ionized peptide fragments with experimentally obtained spectra to identify the presence of specific S-S bonds.

Problem Statement

Following the improvements in mass spectrometry, MS-based methods generally outperform methods using sequence-based learning formulations, as showed by Lee and Singh [3]. However, a number of algorithmic challenges remain outstanding in realizing the potential of MS-based approaches. Salient among these are: (1) *accounting for multiple ion types in the data* [4, 5]: To avoid an exponential increase in the search space, a common simplification is to limit the analysis to the spectra of *b*-ions and *y*-ions only. However, this simplification may erroneously ignore the occurrence of other ions, such

as: *a*, b^o, b^*, *c*, *x*, y^o, y^*, and *z*. (2) *Design of efficient search and matching algorithms*: The search space of possible disulfide topologies increases rapidly not only with the number of ion types being analyzed but also with the number of cysteines as well as the types of connectivity patterns. Thus, it is imperative to have algorithms that can accommodate the richness of the entire problem domain. (3) *Automated data-driven determination of parameters:* Many advanced algorithms in this area are intrinsically parametric. Often, determining the optimal value of these parameters automatically is in itself, a complex problem. This places the practitioner at a significant disadvantage. Support for automated and data-driven strategies for estimation of crucial parameters is therefore crucial to the real-world success of a method in this problem domain. *(4) Addressing the limitation of MS-based approaches:* Although MS-based approaches are powerful methods for determining disulfide connectivity, it fails when the MS/MS spectra contains *blind spots*. A *blind spot* occurs when the precursor ion fragmentation produces different fragments only at the outside boundaries (A) of the intra-disulfide bond or (B) of the inter-chain cross-linked disulfide bonds. This can cause too few product ions to be generated; thus the limited information can prevent accurate determination of disulfide bonds using MS-based methods.

The contributions of this work in context of the aforementioned challenges include: (1) Development of a highly efficient strategy for multi-ion disulfide bond analysis by considering *a*, *b*, b^o, b^*, *c*, *x*, *y*, y^o, y^*, and *z* ion types. To the best of our

knowledge, this is the first algorithmic work that has considered all these ion-types in S-S bond determination. (2) A fully polynomial-time algorithm that selectively generates only those regions of the search space where the correct solutions reside with a high likelihood. (3) A multiple-regression-based data driven method to calculate the critical parameters modulating the search, so as to ensure that the correct bonding topologies are not missed due to the truncation of the search space. At the same time, the parameter selection ensures that the search is focused on the most promising regions of the search-space. (4) A local-to-global strategy that builds a globally consistent bonding pattern based on MS data at the level of individual bonds. (5) Assignment of probability-based scores [6] to each specific disulfide bond based on the number of MS/MS matches and their respective abundance. These scores represent an assessment of quality and reflect the significance of the disulfide bond and (6) Fusion of predictive techniques with the MS-based method to address the limitations imposed by "spotty" MS/MS spectra. This novel approach represents a break-through in the determination of disulfide bonds. It combines the efficiency of MS-based methods with the autonomy of predictive techniques, creating a method which is able to determine the disulfide connectivity of proteins with high accuracy.

Review of Prior Work

In this section, different applications developed to determine proteins disulfide connectivity based on either sequence-based connectivity prediction or mass spectrometry data S-S bond identification are reviewed. First, it is important to note that a disulfide linkage pattern can be represented by an undirected graph, where the set of vertices correspond to the set of bonded cysteines and every edge corresponds to a disulfide bond. This motivated the work from Fariselli and Casadio [7-9]. They used a graph-based approach to determine the disulfide linkage by solving the maximum weight matching problem. From a completely connected graph G formed by v vertices corresponding to the v cysteines and $(v \times (v-1)/2)$ edges with non-zero weights corresponding to possible disulfide bonds, the disulfide connectivity was defined as the solution of the maximum weight matching problem on G.

Another sequence-based connectivity prediction method was developed in [10]. Vullo and Frasconi used recursive neural networks (RNN) for scoring labeled undirected graphs that represented disulfide bond connectivity patterns. RNN outperformed the work of Fariselli and Casadio because RNN allowed the addition of evolutionary information, incorporating multiple alignment profiles in the graphical representation of disulfide connectivity patterns. The used of RNN led the way of the DISULFIND prediction server [11]. DISULFIND uses a combination of machine learning algorithms to predict intra-

chain bridges from the protein sequence alone. It solves the prediction problem in two steps. First, the bonding state of each cysteine is predicted by a SVM binary classifier. Next, cysteines known to participate in the formation of S-S bonds are represented in an undirected graph whose vertices are cysteines and the edges are disulfide bridges. The most probable connectivity pattern is found by the use of a recursive neural network.

Ferre and Clote [12-13] used secondary structure information and diresidue frequencies to develop their web server called DiANNA using a three-step procedure. First, a neural network was trained to recognize cysteines in an oxidized state (sulphur covalently bonded) as distinct from cysteines in a reduced state (sulphur occurring in reactive sulfhydryl group SH). The neural network input is a window of size *w* centered at each cysteine in the sequence. The second neural network is used to score each pair of symmetric window from the previous step. This time, the network input contains evolutionary information obtained by the use of PSIBLAST [14] and PSIPRED [15]. Finally, the algorithm calculates the maximum weight matching (similar to the approach implemented by Fariselli and Casadio) of the formed undirected graph (output from the second neural network) to infer the most probable disulfide bond connectivity.

Zhao *et al.* [16] used cysteine separations profiles (CSPs) to infer disulfide connectivity of proteins. The method is based on the assumption that two proteins with similar cysteine separations share the same disulfide connectivity [17]. For a protein with

n disulfide bonds and *2n* cysteines residues, a cysteine separations profile is defined as $CSP^X = (s_1, s_2, \ldots, s_{2n-1}) = (C_2 - C_1, C_3 - C_2, \ldots, C_{2n} - C_{2n-1})$, where C_i is the position of the *i*th cysteine in protein *X* and s_i is the separation between cysteines C_i and C_{i+1}. This method searches in a protein database (with annotated disulfide bonds) for a correspondence (of a given protein) that has the most similar cysteine separations and returns its disulfide connectivity. The most resembled CSPs are identified by the divergence *D* between them. *D* is defined as $D = \sum_i |s_i^X - s_i^Y|$, where s_i^X and s_i^Y are the *i*th separations for CSPs of two proteins *X* and *Y*.

CSPs were also used by Tsai *et al.* [18] in the development of the application PreCys. This work outperformed the aforementioned methods by using another machine learning technique: support vector machine (SVM) to define the connectivity potential between cysteines. Two descriptors were used to train the SVM: a local sequence profile and CSP. The disulfide linkage was found by solving the maximum weight matching problem for an undirected graph formed by vertices (cysteines) and edges (S-S bonds) found by the trained SVM.

SVMs allowed Chen *et al.* [19] to obtain even better results (70% accuracy) using two-level SVM models. The idea of the two-level framework is to extend the modelling from a local view (pair-wise) to a global perspective (pattern-wise). The first level

focuses on the relationship between two cysteine residues to infer the bonding probability between cysteine pairs. The second level combines the results from the first level with global information of proteins, such as CSPs, cysteines ordering and protein length to predict the disulfide connectivity.

In the following, MS-based methods for disulfide bond determination are reviewed. At the state of the art, Mass Spectrometry became the primary method for protein identification. The basic strategy for determining disulfide bonds using mass spectrometric data consists of three main steps: (1) a protein mixture is cleaved using specific proteases such as trypsin, chymotrypsin or endoproteinase GluC. Next, the digested peptides are separated and analyzed by an ionization method. The most common ionization methods are Electrospray ionization (*ESI*) or matrix-assisted laser desorption/ionization (*MALDI*). These techniques allow peptides and protein molecular ions to be put into the gas phase without fragmentation. These ions in the gas phase are then fragmented by a specific dissociation method. Some of the most common dissociation methods are: collision induced dissociation *(CID)*, electron capture dissociation (*ECD)*, electron transfer dissociation (*ETD)* and electron-detachment dissociation (*EDD)*. (2) The fragments generated by the previous techniques, called precursor ions, are fragmented into smaller fragments called product ions. Each precursor ion is responsible for generating a spectrum of product ions. (3) The entire spectra generated in the previous step are thus compared to spectra from genomic databases that

can be searched using mass spectrometry data. Finally, the correspondences founds are used to determine the disulfide bond connectivity of the protein being analyzed.

MS2Assign/MS2Links [20-21] is one of the earlier implementations of a MS-based method to determine disulfide connectivity. In it, the input consists of the peptide amino acid sequences, a text file containing a list of singly-charged product ion peaks to assign, the site of crosslinking and/or modification for each peptide, the mass shift due to the crosslinking and/or modification reagents, the mass type (monoisotopic or average) and the error threshold used to make the assignments. With this information, MS2Assign generates a theoretical library, constructed based on common peptide fragmentation pathways, containing all the possible fragmentation products and assigns the product ions list. MS2Assign thus attempts to assign each product ion peak obtained in a MS/MS experiment to a product ion in the fragmentation library to within a user-defined error threshold. Its main limitations are: (1) the accuracy of method is outperformed by the newer developed methods, (2) it does not contain a user-friendly interface and the parametric input is not straightforward, (3) only supports one crosslink per peptide or pair of peptides and (4) does not consider the fragmentation products generated from cleavages within the crosslinker itself.

Lee and Singh [3, 22-23] implemented another MS-based method called MS2DB, which forms the basis of the work developed here. The MS2DB framework is mainly

divided in three steps: (1) precursor ions formed from the fragmentation of proteins (MS-data) are matched with a theoretically created library of fragments based on the protein primary amino acid sequence, the protease used to cleave the protein and a specified number of missing cleavage sites. (2) Each match found in the previous step is further analyzed. This second step seeks to validate all the initial matches. Due to the exponential characteristics and variability of the search space, matches could be found randomly by chance. (3) Once all the initial matches are validated, the most probable disulfide bond connectivity pattern is determine by solving the maximum weight matching problem for an undirected graph where the possibly bonded cysteines represent the vertices and all the practical disulfide bonds found in the previous step represent the edges (with non-zero weights) in the graph. Results from [3] showed that MS2SB outperformed MS2Assign while analyzing a set of nine proteins.

Another state-of-the-art MS-based method was developed by Xu *et al.* [24]. MassMatrix is a database search algorithm created to identify disulfide-linked peptides in tandem (MS/MS) data sets. In it, proteins and peptides with disulfide bonds can be identified with high confidence without chemical reduction or other derivatization. MassMatrix has two disulfide search modes: exploratory and confirmatory. In the exploratory search mode, all cysteine residues in the protein sequences are considered to be possible disulfide bonding sites. During searching, MassMatrix will generate all possible combinations of disulfide bonds. In the confirmatory search mode, only the

disulfide bonds specified in the protein database by the user will be considered and searched against the experimental data. Once the matches are found, they will be scored according to the quality of the match. MassMatrix also uses a probabilistic score model to aid in the analysis of the disulfide bonds encountered.

Background and Formulation

Definitions

In this section, some of the general terms and entities used to describe MS-based methods to determine the disulfide connectivity of proteins are defined. These definitions are crucial for the understanding of the concepts and techniques presented hereafter.

Definition 1: Amino acids are molecules containing an amino group, a carboxylic acid group and a side chain that varies between amino acids. There are twenty different natural amino acids and each one is defined by its side chain (represented by the letter R on Figure 2).

Figure 2 – The general structure of an amino acid

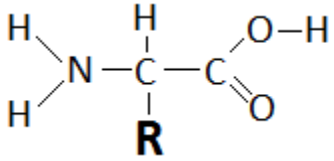

Definition 2: A protein (also known as polypeptide) is an organic compound made of amino acids arranged in a linear chain and folder into a globular form. The amino acids in a polypeptide chains are linked by peptide bonds. Once linked, these amino acids can also be referred to as residues. The linear chain for the protein Lysozyme (Swiss-Prot ID: P00698) is shown in Figure 3.

Figure 3 – Lysozyme polypeptide chain (148 amino acids long)

```
        10         20         30         40         50         60
MRSLLILVLC FLPLAALGKV FGRCELAAAM KRHGLDNYRG YSLGNWVCAA KFESNFNTQA

        70         80         90        100        110        120
TNRNTDGSTD YGILQINSRW WCNDGRTPGS RNLCNIPCSA LLSSDITASV NCAKKIVSDG

       130        140
NGMNAWVAWR NRCKGTDVQA WIRGCRL
```

Definition 3: A cysteine (abbreviated as **C**) is an hydrophobic alpha amino acid, whose codons are UGU and UGC. The side chain on a cysteine is a thiol (-SH). The cysteine (Figure 1) is the only amino acid which may form disulfide bonds.

Definition 4: A cysteine-containing peptide (*CCP*) is a peptide chain containing at least one cysteine residue. A *CCP* with *n* cysteine residues might participate in up to *n* disulfide bonds, since each cysteine may participant in up to one S-S bond. Cysteine-containing peptides are the only (essential) peptides required in the disulfide bond connectivity determination by MS-based methods.

Definition 5: A disulfide bond (also known as S-S bond or disulfide bridge) is a covalent bond derived from the oxidation of two thiol groups (Figure 1). Although a disulfide bond connects the side chains of two different cysteines, they are stronger than peptide bonds. Therefore, the mass spectrometry fragmentation process generally breaks peptide bonds, while S-S bonds most often stay intact.

Definition 6: A mass spectrometer is an instrument that measures the mass-to-charge ratio of ions formed from molecules. With the ions mass-to-charge ratio, the masses of individual molecules can be inferred. This instrument will be detailed in the subsequent section named Mass Spectrometry.

Next, Table 1 contains the key abbreviations used in the ensuing description and their respective definitions.

Table 1 - Abbreviations and their definitions.

Abbreviation	Definition
DMS	Set of mass values corresponding to all possible disulfide-bonded peptide structures that can be obtained from a digested protein.
PMS	Set of mass values of ions that undergo dissociation to produce product ions (set of precursor ions).
IM	Correspondence obtained when the difference between the detected mass of a targeted ion from the *PMS* and the calculated mass of a possible disulfide-bonded peptide structure from the *DMS* is less than a match threshold T_{IM}.
T_{IM}	Initial Match threshold. Threshold used to define a mass window centered on a *PMS* value within which a correspondence between a *DMS* value and a *PMS* value may be found.
ε	*DMS* trimming parameter used to trim the *DMS* set. To trim the *DMS* set by ε means to

	remove as many elements from *DMS* as possible without losing meaningful mass values.
TrimSet	Set of trimmed mass values from the *DMS* set.
PM	Peptide Mass: cysteine-containing peptide mass value.
TempSet	Temporary mass set containing possible disulfide bonded peptide structures.
FMS	Set of mass values of every disulfide-bonded fragment structure that can be obtained from fragment ions, which can be of types a, b, b^o, b^*, c, x, y, y^o, y^* and z.
TMS	Set of mass values of the product ions obtained after the MS/MS step (MS/MS spectra).
VM	Correspondence obtained when the difference between a precursor ion fragment mass from *TMS* and a disulfide-bonded fragment structure mass from *FMS* falls below a validation match threshold T_{VM}.
T_{VM}	Validation Match threshold. Threshold used to define a mass window centered at a *TMS* value in which a correspondence between a *FMS* value and a *TMS* value may be found.
δ	*FMS* trimming parameter used to trim the *FMS* set. To trim the *DMS* set by δ means to remove as many elements from *FMS* as possible without losing meaningful fragment ions mass values.
FragSet	Set containing the mass values of fragment ions generated by the method GENFRAGS(.) in the APROX-FMS routine.

Illustrative Examples

Disulfide bonds are usually formed in the endoplasmic reticulum by oxidation. For this reason, S-S bonds are mainly found in extracellular, secreted and periplasmic proteins, although they can also be formed in cytoplasmic proteins under conditions of oxidative stress [25]. In UniProtKB (also known as SwissProt knowledgebase), two main types of disulfide bonds are annotated: (1) Intrachain disulfide bonds and (2) Interchain disulfide bonds. While intrachain disulfide bonds are formed between two cysteines within the same polypeptide chain, interchain S-S bonds are formed between two

cysteines of individual chains of the same protein or between two cysteines of distinct proteins.

In the following, the presence of disulfide bonds is illustrated by reviewing some examples extracted from SwissProt database. Intrachain disulfide bonds were annotated in the following proteins:

i. Neuroendocrine 7B2 [www.uniprot.org/uniprot/P18844]
ii. Acetylcholine receptor subunit alpha-like 1 [www.uniprot.org/uniprot/P09478]

The protein Neuroendocrine contains an intrachain disulfide bond between cysteines in the positions 73 and 82, respectively. This protein acts as a molecular chaperone for the human protein pcsk2, being responsible for its transport from the endoplasmic reticulum to later compartments of the secretory pathway where pcsk2 is proteolytically matured and activated (preventing its premature activation in the regulated secretory pathway). It is also required in the cleavage of pcsk2; however it does not appear to be engaged in its folding.

Two other intrachain disulfide bonds (between cysteines C^{149}-C^{163} and cysteines C^{222}-C^{223}) are found in the protein Acetylcholine receptor subunit alpha-like 1 (also known as nAcRalpha-96Aa or just AcrB). This protein is found in the fruit fly (*drosophila melanogaster*) and triggers an extensive change in the conformation of the

protein acetylcholine (when bound to it) that affects all subunits and lead to the opening of an ion-conducting channel across the plasma membrane.

Interchain disulfide bonds were found in the following proteins:

i. Bone morphogenetic protein 2-A [www.uniprot.org/uniprot/P25703]
ii. Histone H3.1 [www.uniprot.org/uniprot/P68432]

Three inter-chain S-S bonds were annotated for the protein bone morphogenetic 2-A (between cysteines C^{298}-C^{363}, C^{327}-$C^{395}$and C^{331}-C^{397}). This protein induces cartilage and bone formation in African clawed frogs (*xenopus laevis*). Another interchain disulfide bond was found in the protein histone H3.1 present in bovines (*bos taurus*). This protein is a core component of nucleosomes. Nucleosomes wrap and compact DNA into chromatin, limiting the DNA accessibility to the cellular machineries which require DNA as a template. Histones play a very important role in transcription regulation, DNA repair, DNA replication and chromosomal stability. More examples showing the presence and importance of both intrachain and interchain disulfide bonds will be presented in the forthcoming Experiments section.

Mass Spectrometry

The idea underlying Mass Spectrometry dates back over a century when JJ Thomson invented the vacuum tube when the existence of electrons and “positive rays” was demonstrated. At that time, Thomson observed that his discovery could be used

profitably by chemists to analyze chemicals. However, the application of mass spectrometry remained in the realm of physics for nearly thirty years [26]. Then it was used to discover a number of isotopes, to determine the relative abundance of the isotopes and to measure their mass values within a precision of 1 part in 10^6. These measurements laid the basis for later developments in diverse fields ranging from geology to biochemical research.

Mass Spectrometry is a powerful analytical technique used to identify unknown compounds, to quantify known compounds and to elucidate the structure and chemical properties of molecules. One of the advantages of mass spectrometry is that it can identify compounds with very minute quantities at very low concentrations (one part in 10^{12}). Mass spectrometry provides valuable information to many different areas and professionals, such as bioinformaticians, chemists, physicians, astronomers, biologists, nutritionists and geologists. Among others, mass spectrometry can be used to: (1) locate oil deposits by measuring petroleum precursor in rock, (2) establish the elemental composition of semiconductor materials, (3) monitor fermentation processes for the biotechnology industry and (4) determine whether honey is adulterated with corn syrup. According to the American Society for Mass Spectrometry, mass spectrometry can also be employed in:

- determine how drugs are used by the body

- perform forensic analysis such as conformation and quantification of drugs abuse
- analyze environmental pollutants
- determine the age and origins of specimens in geochemistry and archaeology
- perform ultrasensitive multi-element inorganic analyses

The core instrument in a mass spectrometry experiment is the mass spectrometer. It measures the masses of individual molecules that have been charged and converted into ions. Since molecules are so small, it is infeasible to measure their mass in grams, pounds or kilograms (i.e. the mass of a hydrogen atom is approximately 1.66×10^{-24} grams). The unit of mass used by chemists is called Dalton or Da and is defined as 1/12 of the mass of a single atom of the isotope of carbon-12 (^{12}C). Thus, the isotope ^{12}C weights 12Da or 12 mass units. In reality, the mass spectrometer does not measure the molecular mass directly, but rather the mass-to-charge ratio of the ions formed from molecules. The charge unit used is the fundamental unit of charge, the magnitude of charge on an electron. Therefore the measured mass-to-charge value (also known as m/z value) corresponds to the number of Daltons per fundamental unit of charge.

The size of a mass spectrometer ranges from a home microwave size to instruments that occupy entire research labs. A blocks diagram representing the components of a mass spectrometer as well as the other instruments used in a mass spectrometry experiments is presented in Figure 4. The formation of gas phase ions is an essential prerequisite to the mass sorting and detection processes that occur in a mass

spectrometer. Nowadays, initial samples may be solid, liquid or vapor. These samples will vary according to the inlet and ionization techniques used in the mass spectrometry experiment. At the end of the ions source, the entire sample will be transformed in gas phase ions. These ions will be sorted in the mass analyzer according to their mass-to-charge (m/z) ratios and then collected by an ions detector. There, the ions flux is converted to a proportional electrical current. Finally, the data system records the magnitude of these electrical signals as a function of m/z and converts the information into a mass spectrum. A mass spectrum is a graph of relative ion intensity as a function of the mass-to-charge ratio.

Figure 4 – The components of a mass spectrometry experiment

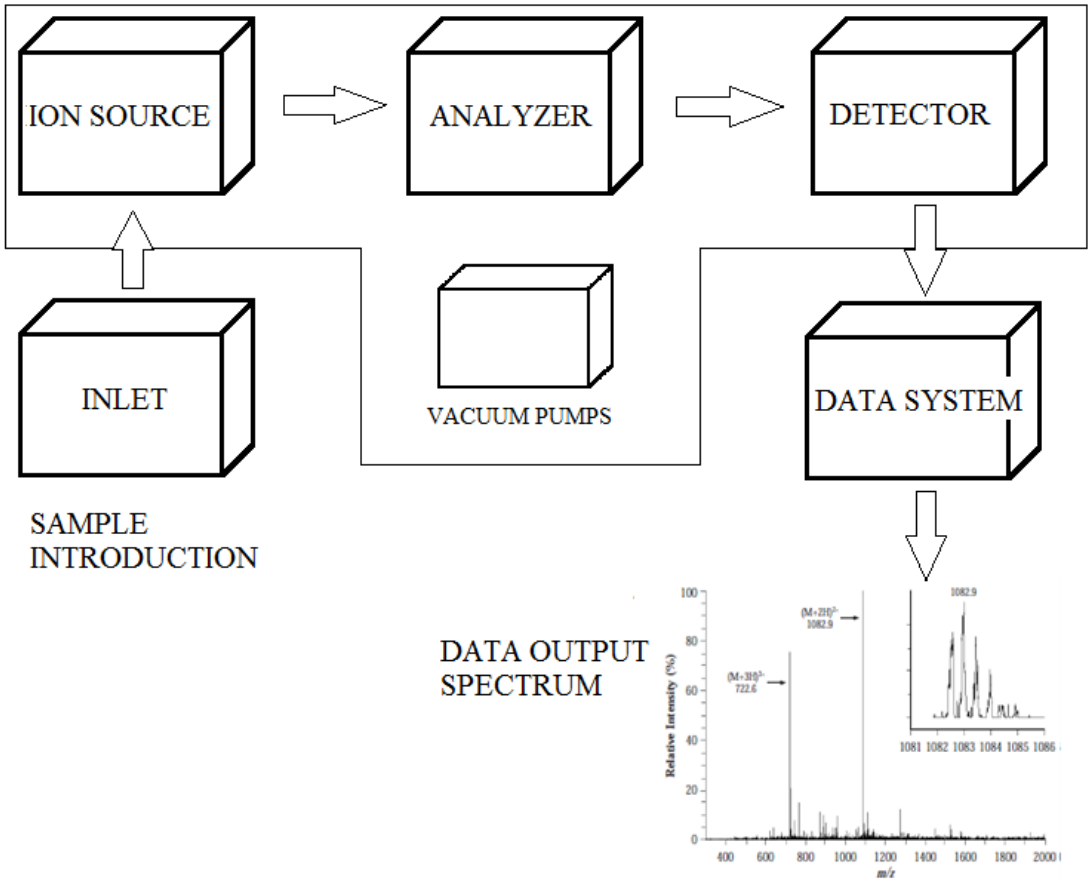

When a mixture (in the solid, liquid or gas phase) is analyzed, the individual components must be separated prior to analysis by mass spectrometry. This separation is required for unambiguous classification, since different compounds might create an overlapping or mixed spectrum. This problem is resolved by the coupling of gas chromatography, liquid chromatography or capillary electrophoresis devices to the mass spectrometer in order to separate components of complex mixtures prior to the mass analysis.

At the ion source, ions can be generated in different ways. One method is by bombarding the gaseous sample molecules with a beam of energetic electrons. This process is called electron ionization (EI). Another method is called electrospray ionization (ESI) and consists of using electricity to disperse a liquid or the fine aerosol resulted in this process. ESI is usually coupled with Liquid chromatography (LC-ESI) and is the method of choice in biological and pharmaceutical analysis, since it can add many charges to the protein molecules, allowing large molecules to be analyzed by mass spectrometer with a m/z range of only 2000. The energy used to ionize the compounds is generally much greater than the energy of most of the bonds which hold the molecule together (one exception is the disulfide bond); therefore, not only ionization occurs but bonds are broken and fragments are formed. All the neutral molecules and neutral fragments existing in this final mixture are removed, since they won't produce any meaningful results. In both of these ionization processes, positive-ion mass spectra are most commonly recorded, because fewer negative ions are formed. Therefore, while positive ions are propelled to the analyzer, negative ions are trapped and further discarded.

The analyzer uses dispersion or filtering to sort ions according to their mass-to-charge ratios or a related property. The most common analyzers are magnetic sectors, quadrupole mass filters, quadrupole ion trap, Fourier transform ion cyclotron resonance spectrometers, and time-of-flight mass analyzers. Magnetic sectors bend the trajectories

of ions into circular paths of radii which directly correlate to their m/z ratio. Ions of larger m/z follow larger radius paths, whereas ions of smaller m/z follow smaller radius paths. A slit is then used to filter ions with the desired m/z ratio. A quadrupole mass filter analyzer sorts the ions by applying different field strengths, thereby changing the m/z value that is transmitted to the detector. The quadrupole ion trap operates based on a similar principle. However, in this case the ions are trapped into a ring electrode for subsequent analysis. The different m/z values are indirectly measured by the voltage applied to the electrode required to release the ions from the trap.

In an FT-ICR analyzer, ions are trapped electrostatically within a cubic cell in a constant magnetic field. A covalent orbital (defined as a cyclotron) motion is induced by the application of a radio-frequency (RF) pulse between the excite plates. The orbiting ions generate a faint signal in the detect plates of the cell. The frequency of the signal from each ion is equal to its orbital frequency, which is inversely related to its m/z value. The signal intensity of each frequency is proportional to the number of ions having that m/z value. The signal is amplified and all the frequency components are determined, yielding the mass spectrum. Finally, time-of-flight analyzers classify ions based on their different flight times over a known distance. After a small amount of ions are emitted from a source, they are accelerated so that ions of like charge have equal kinetic energy. Next, this group of ions is directed into a flight tube. Since kinetic energy is equal to

$E_k = \frac{1}{2}mv^2$, where *m* is the mass of the ion and *v* is the ion velocity, the lower the ion's mass, the greater the velocity and consequently the shorter the flight time. The time of flight of ions, measured in microseconds, can be transformed to their respective m/z values using the formula above.

The detector used after the Fourier transform ion cyclotron resonance analyzer measures the oscillating signal induced by orbiting ions in the detect plates to detect the targeted ions. For all other analyzers, the ions are detected after mass analysis by converting the detector-surface collision energy of the ions into emitted ions, electrons or photons that are measured with different light or charge sensors. The block Data System in Figure 4 represents both computer hardware and software used to acquire the data, store, analyze and present it in the form of mass spectra in different file formats.

The analysis refinement (better identification) of complex samples is achieved by the coupling of two or more stages of mass analysis. When two stages are coupled, the experiment is entitled mass spectrometry/mass spectrometry (MS/MS), also known as tandem mass spectrometry (tandem MS/MS). In a tandem MS/MS experiment, the first mass analyzer selects ions of a specific m/z value to be further fragmented. These ions, described as precursor ions or parent ions, go through a second mass analyzer, which

generates product ions (fragments of the precursor ion). Lastly, these product ions are detected and a mass spectrum is generated for each precursor ion selected.

Blind Spot

A blind spot is a region in a tandem MS/MS mass spectrum in which fragments (peaks) with relevant intensity cannot be found (are not generated) during the mass spectrometry experiment. A blind spot occurs when (1) the precursor ion fragmentation produces different fragments only at the outside boundaries of the intra-disulfide bond, (2) the presence of cross-linked or circular disulfide bonds prevent the fragmentation of precursor ions or (3) the energy used to fragment complex molecules is not enough to break strong intrachain and interchain bonds present in the molecules structure. This can cause too few product ions to be generated. Unfortunately this limited information can prevent accurate determination of disulfide bonds using MS-based methods. This restriction motivated the novel idea to use predictive techniques, in combination with MS-based methods, to predict the disulfide bonds in these “blind spot regions”, where only MS-based methods would fail to determine S-S bonds. The results obtained and discussed in the Experiments section prove the validity of the approach.

Method

A diagrammatic representation of the key steps of a MS-based method for disulfide linkage determination is presented in Figure 5, along with the different types of fragment ions that can be generated as an outcome of this process. One of the novelties in the method developed is the consideration of ten different ion types: *a*, *b*, b^o, b^*, *c*, *x*, *y*, y^o, y^*, and *z* in the analysis of MS/MS data. Figure 6 shows in greater details the presence of multiple ion types in different MS/MS spectra for two proteins: Lysozyme and Pratelet glycoprotein 4.

Figure 5 - (A) Once a protein is digested, the theoretically possible disulfide bonded peptides are compared with experimentally obtained precursor ions. In order to confirm each correspondence, the possible disulfide bonded fragment ions are next compared with experimentally generated MS/MS spectra. (B) Most of the different fragment ions (and their nomenclature) that can be observed. Ions types not represented here include *b* and *y* ions which have either lost a water molecule (b^o, y^o) or have lost an ammonia molecule (b^*, y^*).

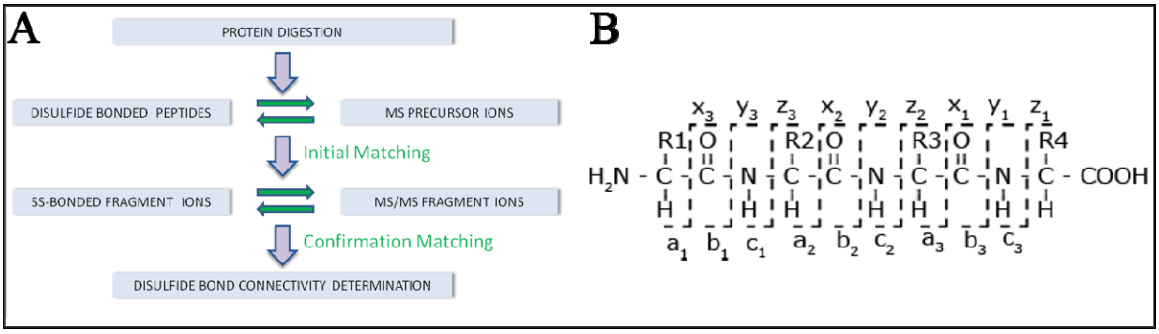

Figure 6 - Presence of multiple ions types (in green) after *CID*. In the first spectrum, note the presence of b^o and y^o ions with high intensity in the fragmentation of the precursor ion whose sequence is FFLQGIQLNTILPDAR, for the protein Lysozyme

[Swiss-Prot: P11279]. In the second spectrum, *a*, b^o, b^*, and y^o ions (all with high intensity) can be observed after the fragmentation of a precursor ion existing in the protein Pratelet glycoprotein 4 [Swiss-Prot P16671].

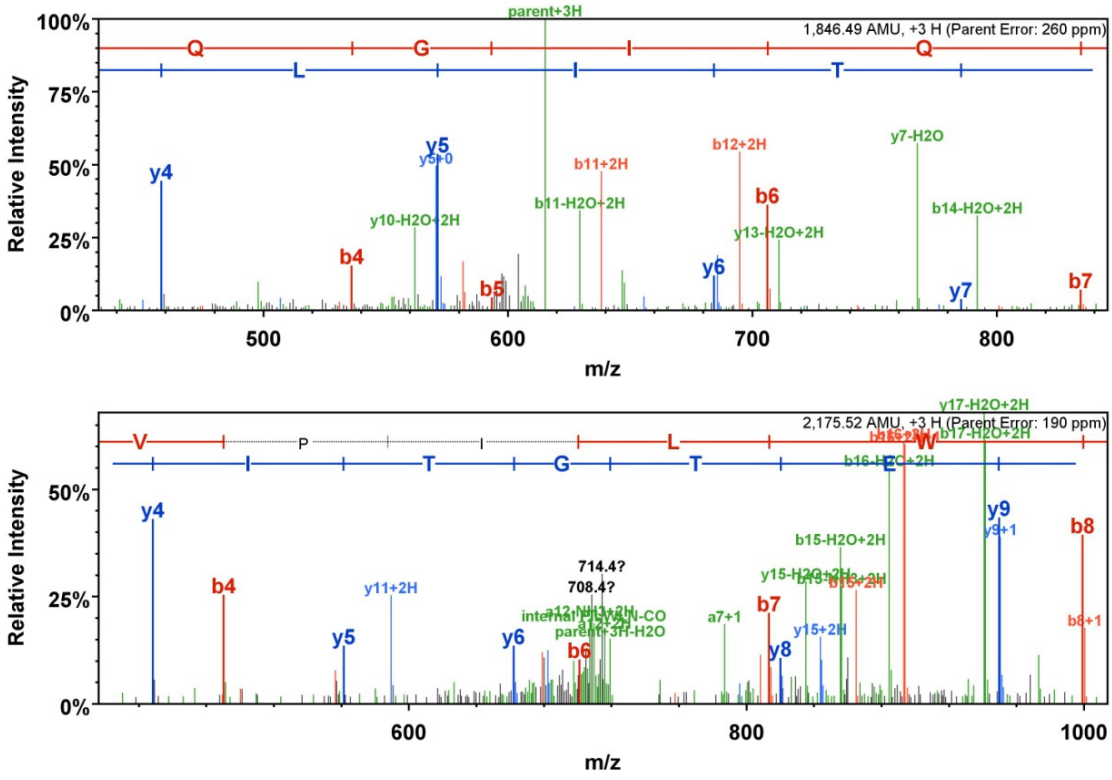

At a high-level, the proposed approach can be thought of as a two-stage database-based matching technique (see Figure 7). During the first stage, the mass values of the theoretically possible disulfide-bonded peptide structures are compared with precursor ion mass values derived from the MS-spectra. In the second (confirmatory) stage, the theoretical spectra from the disulfide-bonded peptide structures are compared with MS/MS experimental spectra. The confirmatory step is necessary since a disulfide

bonded peptide may not actually correspond to a precursor ion, even if their mass values are similar. This approach allows us to conduct the entire search process in (a low degree) polynomial time.

Figure 7 – Two-stage matching spectra for protein ST8SiaIV. (A) In the first-stage (*DMS* vs. *PMS*), the theoretical disulfide-bonded structure is matched with the doubly charged precursor ion with highest intensity, whose *m/z* = 1082.9. (B) For this initial match, the disulfide-bonded peptide pair is fragmented and the fragments are matched with the MS/MS spectrum for the precursor ion (*FMS* vs. *TMS*), generating a list of validation matches.

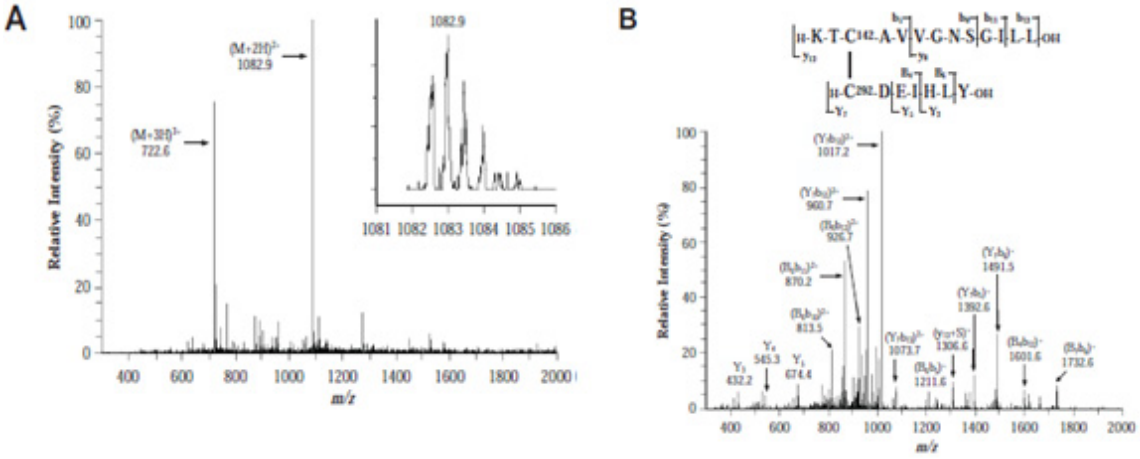

In the first stage of the method, an *Initial Match* (*IM)* is characterized when the difference between the detected mass of a targeted ion from the *PMS* and the calculated mass of a possible disulfide-bonded peptide structure from the *DMS* is found to be less than a threshold T_{IM}. The second stage validates (or rejects) the initial matches. For each Initial Match, the validation occurs by searching for matches between product ions from the *TMS* and the theoretical spectra *FMS*. A *Validation Match* (*VM*) is said to occur when

the difference between a precursor ion fragment mass from *TMS* and a disulfide-bonded fragment structure mass from *FMS* falls below a validation match threshold T_{VM}.

Unfortunately, the sizes of both *FMS* and *DMS* grow exponentially. For a disulfide-bonded peptide structure consisting of k peptides, considering that there are f different fragment ion types possible, up to f^k types of fragment arrangements may occur in the *FMS*. If the ith fragment ion consists of p_i amino acid residues, then the complexity to compute the entire *FMS* for a disulfide-bonded peptide structure is $O\left(f^k \times \prod_{i=1}^{n} p_i\right)$ using a brute-force approach. The *DMS* also grows exponentially. To understand this, let $P = \{p_1, p_2, \ldots, p_k\}$ be the list of cysteine-containing peptides in a polypeptide chain. Further, let $C = \{c_1, c_2, \ldots, c_i\}$ be the list of the number of cysteines per cysteine-containing peptide p_i. If $n = \sum_1^i c_i$ is the total number of cysteines in a protein, the number of possible disulfide connectivity patterns (*DMS* size) is: $(n-1)!! = \prod_{i=1}^{n/2} (2i-1)$.

The subset-sum formulation: Towards polynomial-time matching

Given the growth characteristics of the *DMS* and the *FMS*, an exhaustive search-and-match strategy is clearly infeasible in the general case. This is especially true if multiple ion types are considered. The approach developed towards designing an efficient algorithm for this problem is based on the key insight that the *entire search space (DMS or FMS) does not need to be generated to determine the matches*. That is, the method

only generates the few disulfide bonded peptides whose mass is close to the (given) experimental spectra rather than generate all possible peptide combinations and subsequently testing and discarding most of these. This insight allows the *DMS* and *FMS* generation to be re-casted as instances of the subset-sum problem [27]. Recall, that given the pair (*S*, *t*), where *S* is a set of positive integers and $t \in \boldsymbol{Z}^{+}$, the subset-sum problem asks whether there exists a subset of *S* that adds up to *t*. While the subset-sum problem is itself NP-Complete, it can be solved using approximation strategies to obtain near-optimal solutions, in polynomial-time [27].

Polynomial time DMS mass list construction

The strategy employed lies in obtaining an approximate solution to the subset-sum problem by trimming as many elements from *DMS* as possible based on a parameter ε. To trim the *DMS* set by ε means to remove as many elements from *DMS* as possible such that if DMS^{*} is the resultant trimmed set, then for every element DMS_i removed from *DMS*, there will remain an element DMS_i^{*} in DMS^{*} which is "sufficiently" close in terms of its mass to the deleted element DMS_i. Specifically,

$$(DMS_i / 1+\varepsilon) \le DMS_i^{*} \le DMS_i \qquad (1)$$

Figure 8 - Pseudo code for APROX-DMS and TRIM routines.

```
01. APPROX-DMS (CCP, PMS_val, ε, T_IM)
02.     DMS_0 ← {0}
03.     IM ← { }
04.     TrimSet ← { }
05.     for i ← 0 to (|| CCP || – 1)
06.         PM ← CCP_i
07.         TempSet ← { }
08.         DMSsize ← || DMS ||
09.         for j ← 0 to (DMSsize – 1)
10.             if ((PM + DMS_j) ≤ (PMS_val + T_IM))
11.                 TempSet_j ← PM + DMS_j
12.         DMS ← MERGE (DMS, TempSet)
13.         DMS, Trimset ← TRIM (DMS, TrimSet, ε)
14.     if ((DMS_max) ≥ (PMS_val - T_IM))
15.         IM ← DMS_max
16.     return {IM, DMS, TrimSet}

17. TRIM (DMS, TrimSet, ε)
18.     n ← | DMS |
19.     max_value ← DMS_n-1
20.     last ← max_value
21.     for i ← n-2 down to 0
22.         if last > (( 1+ ε )× DMS_i)
23.             DMS* ← DMS_i
24.             last ← DMS_i
25.         else
26.             TrimSet ← DMS_i
27.     DMS* ← max_value
28.     return {DMS*, TrimSet }
```

The approximation algorithm for creating the partial *DMS* is described by the APPROX-DMS and TRIM routines (Figure 8). APPROX-DMS takes the following parameters: (1) a sorted list of cysteine-containing peptides mass values (*CCP*), (2) a target mass value from the *PMS* list (PMS_{val}), (3) the trimming parameter ε, and (4) the Initial Match threshold (T_{IM}). In lines 2-8 of Figure 8, all the variables and data structures are initialized. In lines 9-11, the theoretical disulfide-bonded peptide structures are formed and stored in a temporary set called *TempSet*. Line 10 excludes values greater than the PMS_{val} plus a constant corresponding to the Initial Match threshold. The rationale behind this threshold is explained in the following section. In other words, the conditional clause in line 10 filters peptide combinations that will not generate any feasible initial match. Line 12 increments the *DMS* by invoking the routine MERGE,

which returns a sorted set formed by merging the two sorted input sets *DMS* and *TempSet*, with duplicated values removed. In line 13, the TRIM routine is called to shorten the *DMS* set. Lines 14-15 examine if the largest mass value in the constructed *DMS* set is sufficiently close to the targeted mass PMS_{val}. If so, an Initial Match occurs.

Table 2 presents an example showing the effectiveness of the APROX-DMS. In this specific case, 37.5% of the entire search space (all feasible combinations of cysteine-containing peptides) was successfully trimmed, while ensuring that the correct *IM* was not missed. Another example illustrating the action of APPROX-DMS on the Beta-LG protein is available in Appendix A.

Table 2 – Running APROX-DMS on the ST8SiaIV C^{142}-C^{292} bond. *CCP*: the mass values of all cysteine-containing peptides. PMS_{val}: a disulfide-bonded precursor ion mass. *TrimSet*: all the disulfide-bonded structures trimmed from the set of feasible combinations of cysteine-containing peptides. For this example, 37.5% of the structures were trimmed and the correct *IM* was found.

Property	Value
CCP	{716, 728, 749, 863, 864, 891, 976, 1096, 1105, 1161, 1204, 1274, 1359, 1367, 1418, 1480, 1593, 1733, 1754, 1846, 1863, 1864, 1976, 2179, 2292, 2351, 2617, 2737, 2822}
PMS_{val}	{2640} *(Precursor $M+H^+$* mass and charge state*: 2638.121 3)*
ε	0.02530
T_{IM}	1.0
TrimSet	*{716, 863, 1096, 1443, 1589, 1590, 1611, 1725, 1832, 1838, 1844, 1853, 1866, 1888, 1909, 1958, 1995, 2001, 2022, 2051, 2066, 2070, 2086, 2094, 2107, 2135, 2164, 2178, 2221, 2248, 2249, 2307, 2333, 2363, 2462, 2519}*
IM	{2640} *(KTCAVVGNSGILL – ATRFCDEIHLY) – SS-bond: C^{142}-C^{292}*

The complexity of both routines MERGE and TRIM is $O(|DMS|+|TempSet|)$ and $O(|DMS|)$, respectively. Further, for any fixed $\varepsilon > 0$, our algorithm is a $(1+\varepsilon)$-approximation scheme. That is, for any fixed $\varepsilon > 0$, the algorithm runs in polynomial time. The proof of the polynomial time complexity of APPROX-DMS can be obtained by direct analogy to the proof of the polynomial time complexity of the subset sum approximation algorithm from [27] and is outlined in Appendix B.

Parameters Estimation

APPROX-DMS depends on two important parameters, namely, the match threshold T_{IM} and the trimming parameter ε. The match threshold is responsible for defining a "matching window". This is necessary due to practical considerations such as the sensitivity of the instrument (i.e. 0.01Da, 0.1Da, and 1.0Da) and experimental noise, due to which an exact match is a rarity. An empirical study was conducted by using different values of T_{IM} for all the datasets. Based on the results, the T_{IM} value of $\pm 1.0Da$ was found to minimize missing matches as well as the occurrence of false positives. Considering the smallest precursor ion mass involved, in these studies, the above value of T_{IM} guaranteed a matching accuracy of 99.86%.

The second parameter ε is much more important as it is crucial to the running time of the algorithm and its accuracy as evident from Eq. (1). To determine ε, we note

that it is inversely proportional to the algorithm's running time. However, a large value of ε would cause meaningful fragments to be left out of the *DMS*. At the same time, a small value for ε will lead to few data points being trimmed. Thus "guessing" appropriate values of ε can be complicated and suboptimal choices can significantly impact the quality of the results. This problem of data-driven estimation of ε is addressed using a regression framework where ε is treated as a dependent variable and based on the data, a functional relationship is obtained between it and the other (independent) variables. This functional relationship is modeled using the following independent variables: (1) the cysteine-containing peptides (*CCP*) mass range defined by CCP_{max} and CCP_{min} corresponding to the peptides with the highest and lowest mass respectively. (2) The number of cysteine-containing peptides *k*. A large *k* implies that the average difference in the mass of any two peptide fragments is small. Conversely, a small *k* implies fewer fragments with putatively larger differences in their masses. (3) The cysteine-containing peptides average mass value $CCP_{average}$. The relationship between ε and these other variables is then obtained using multiple-variable regression. In these studies, the data for the regression was obtained using bootstrapping where groups of four proteins were randomly picked from the set of 9 proteins available to us. The functional relationship defining ε was obtained to be:

$$\varepsilon = 1.3939\times10^{-2} \times \frac{\left(CCP_{\max} - CCP_{\min}\right)}{CCP_{average}} - 1.0824\times10^{-3} \times k + 3.9094\times10^{-2} \qquad (2)$$

Polynomial time FMS construction

In creating the *FMS*, a strategy similar to the one used for generating the *DMS* can be used. This involves using an approximation algorithm, this time, to generate the theoretical spectra for all the *IMs* found during the first-stage matching. Another trimming parameter δ is defined to trim the *FMS* mass list. It can be expected that the functional form of δ depends on the fragments mass range, as well as their granularity (extent to which fragments are broken down into smaller ions). In a manner similar to the case for estimating ε, a multiple-variable regression was used to obtain the specific functional form for the dependent variable δ in terms of the variables AA_{max} (the largest amino acid residue mass), AA_{min} (the smallest amino acid residue mass), $AA_{average}$ (the average amino acid residues mass), and $||p||$ (average number of amino acid residues per fragment). Bootstrapping was once again utilized, resulting in the relationship shown in Eq. (3).

$$\delta = 6.1744 \times 10^{-3} \times \frac{\left(AA_{\max} - AA_{\min}\right)}{AA_{average}} - 3.0936 \times 10^{-3} \times \left\|p\right\| + 5.0731 \times 10^{-2} \qquad (3)$$

Figure 9 - Pseudo code for APROX-FMS routine.

```
01. APPROX-FMS (peptides, TMS_val, δ , T_VM )
02.     FMS_0 ← {0}
03.     VM ← { }
04.     for i ← 0 to (|| peptides || - 1)
05.         TempSet ← { }
06.         Pep_sequences ← peptides_i
07.         FragSet ← GENFRAGS (Pep_sequences)
08.         for j ← 0 to (|| FMS || - 1)
09.             for k ← 0 to (||FragSet|| - 1)
10.                 if ((FragSet_k + FMS_j) ≤ (TMS_val + T_VM))
11.                     TempSet[ ] ← FragSet_k + FMS_j
12.         FMS ← MERGE (FMS, TempSet)
13.         FMS ← TRIM (FMS, δ )
14.     if ((FMS_max) ≥ (TMS_val – T_VM))
15.         VM ← FMS_max
16.     return { FMS, VM }
```

The pseudocode of the APPROX-FMS procedure used for generating the *FMS* is shown in Figure 9. The function GENFRAGS(.), in line 7, generates multiple fragment ions (a, b, b^o, b^*, c, x, y, y^o, y^*, and z) for peptide sequences in $Pep_{sequences}$, which contains the disulfide-bonded peptides involved in the *IM* being analyzed. Next, for each element in the *FMS* and for each fragment in the *FragSet* (lines 8-11), new disulfide-bonded peptide fragment structures are formed. Line 10 rejects values greater than the TMS_{val} (also considering the Validation Match threshold), since they cannot generate any feasible validation match. In line 12, the current *FMS* set is combined with the disulfide-bonded peptide fragments set *TempSet* using MERGE. In line 13, the *FMS* is trimmed using the TRIM routine. Lastly, a Validation Match *VM* is declared (lines 14-15) when a

correspondence is found between the mass of the largest value in *FMS* and an experimentally determined mass value TMS_{val}, given a Validation Match threshold.

Match score for S-S bonds determined using MS/MS data

Once all Initial Matches are processed, a match score is assigned to each putative disulfide bond found in the validated *IMs*. This score represents the combined importance of each single peak match within two spectra. Each specific peak match is weighted according to its intensity. The match score is given by:

$$V_S = \left(\sum_{i=1}^{n} (VM_i \times I_N) / \sum_{i=1}^{n} (TMS_i \times I_N) \right) \times 100 \qquad (4)$$

In Eq. (4), the numerator corresponds to the sum of each validation match for a disulfide bond multiplied by the matched MS/MS fragment normalized intensity value (I_N). Here, VM_i is a binary value which is set to 1 if a confirmatory match was found for fragment *i*. The denominator similarly contains the sum of each experimental MS/MS fragment ion from *TMS* multiplied by I_N. Here, TMS_i is a binary variable which indicates the presence of a fragment *i* in the MS/MS spectrum.

Integration with predictive techniques

A "local" (putative bond-level) view of the possible disulfide connectivity is formed once all the *Initial Matches* and *Validation Matches* are calculated. Unfortunately however, MS-based disulfide connectivity determination has some constraints which

might prevent the method from finding all disulfide bonds in a protein. Among these limitations, the most impacting one is the presence of blind spots in the MS/MS spectra. As previously mentioned, blind spots may be caused by intra-chain disulfide bonds, cross-linked disulfide bonds and circular disulfide bonds. The different types of disulfide bonds are presented in Figure 10.

Figure 10 – Disulfide bond types. The different S-S bonding types are: (A) inter-chain disulfide bonds, (B) intra-chain S-S bonds, (C) cross-linked disulfide linkages and (D) circular disulfide bonds.

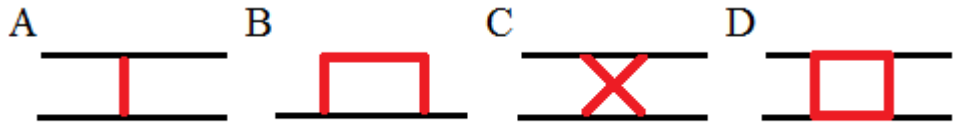

Therefore, a non-MS-based method is necessary to overcome this constraint, since the presence of blind spots occur due to the strength of disulfide bonds, which prevents the fragmentation of the protein during mass spectrometry. Amid possible solutions, predictive techniques were selected to resolve this problem. Motivated by the analysis of the previous work in this area and by results which demonstrated up to 77% accuracy in disulfide linkage determination, a support vector machine (SVM) based framework was implemented.

The framework developed here is based on the work from Chen *et al.* [19]. In their studies, a two-level model was used to predict the disulfide connectivity of proteins.

Results showed that their SVM-based models outperformed all other predictive techniques for disulfide connectivity prediction. The main idea underlying their approach is to combine local and global protein sequence information to train SVM engines, using the strengths of both. While the local information was encoded by pair-wise methods, focused on cysteine pairs, global information was encoded by pattern-wise methods, which took into consideration the different disulfide bonding patterns.

Support Vector Machine (SVM)

Support Vector Machines, or simply SVMs, are a set of supervised learning methods for the classification of both linear and nonlinear data, based on the analysis of information and patterns recognition. SVMs are a non-probabilistic binary classifier, which is a good fit for disulfide bonding determination (since the possible bonding state can be categorized by just two classes). SVMs use a nonlinear mapping to transform the original training data into a higher dimension. Within this new dimension, it searches for the linear optimal separating hyperplane that separates the data into two different classes, creating a decision boundary. With an appropriate nonlinear mapping to a sufficiently high dimension, data from two classes can always be separated by a hyperplane. This hyperplane is found using support vectors and margins [28]. Both entities are represents in Figure 11.

Figure 11 aids in visualization, showing linearly separable 2-D data points, which are divided by a line into two different classes. If an example addressing 3-D data points would be used, the data would be divided by a plane. Generalizing to *n* dimensions, the data points would be separated by a hyperplane. An SVM approaches this classification problem by searching the maximum marginal hyperplane. A maximum marginal hyperplane is defined as the hyperplane with the largest margin. The margin is defined as the distance (or largest separation) between two classes. The diagonal lines traced in black in Figure 11 represent the "sides" of the class division and define two supporting hyperplane. Any data point that falls on these hyperplanes are called support vectors. That is, any support vector is equally close to the maximum marginal hyperplane (in red).

Figure 11 – SVM: representation of a hyperplane dividing data points with two attributes (2-D). The red line corresponds to the maximum marginal hyperplane. The blue arrow shows the margin, while the support vectors are shown with thicker borders.

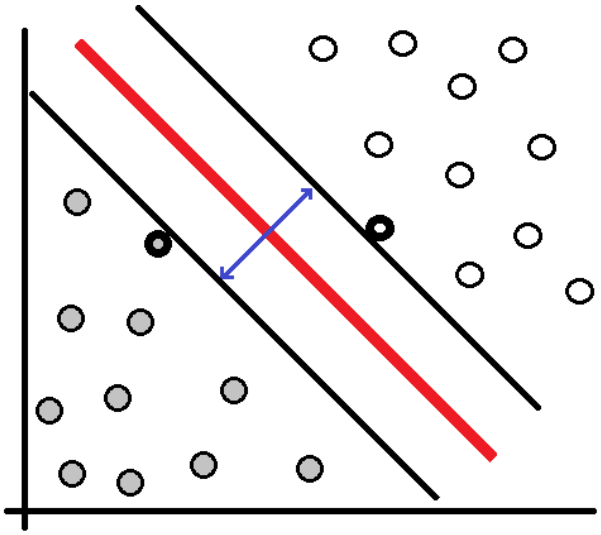

Although the example above uses 2-D data points to facilitate its understanding, SVM is capable of handling data with hundreds or even thousands of different dimensions (attributes). In fact, the SVM trained in this work analyzes data with hundreds of attributes encoded. The proper and complete training of the SVM used specifically in the method, together with the different predictive techniques used to enhance the accuracy of the S-S linkage determination is described next.

SVM-based predictive framework

The fundamental component of properly training a SVM resides in building a robust, accurate and efficient model, based on the training dataset. The same dataset extracted from SWISS-PROT database [25] was employed (denoted as SP43) to compare the framework developed with other approaches [11-12, 18]. A similar filtering procedure to [7] was applied to ensure only high quality and experimentally verified S-S

bond annotations were included. Initially, only the sequences containing information in the Protein Data Bank (PDB) were included in the filtered dataset. In addition, sequences with disulfide annotation described as “probable”, “potential” or “by similarity” were excluded, as well as sequences with more than five disulfide bonds. For cross-validation, the data was further divided into five subsets. Each subset contained an approximately equal number of sequences. The entire filtered dataset contains 439 proteins.

The framework developed can be divided in two levels: pair-wise modeling level and pattern-wise modeling level. Following a similar strategy developed in the MS-based framework, the second stage aims to validate the results obtained from the first stage. In the first level, a SVM model infers the disulfide bonding likelihood between any two cysteines. First, the data were encoded for each possible cysteine pair. For a protein P with D disulfide bonds, there are $D(2D-1)$ combinations of cysteine pairs (i, j) to be encoded. The encoded data was generated by two different descriptors: (1) local sequence profiles around target cysteines and (2) the sequential distance between cysteines (denoted as DOC).

The sequence profiles were extracted using a window centered at cysteines i and j. Each residue in the window covering a cysteine was encoded as a vector of 20 elements, where each element corresponding to an amino acid residue receives a binary value. The element in the vector associated with the amino acid residue is set to 1, while all the other

positions in the vector are set to 0. The window size was set to 13, similarly to the size used in [19] (which was proved to obtain the best predictive results). Since the sequence separation between bonded cysteines correlates with specific connectivity patters as shown in [29], the second descriptor encodes the normalized linear distance between two cysteines *i* and *j*. DOC is defined as $\|i - j\|$, where *i* and *j* represent the indices of two disulfide bonded cysteines. The calculated distance is normalized due to the unitary characteristic of the encoded sequence profile data vectors. The normalization is obtained by the equation $min(DOC/100, 1)$.

Once the data is fully encoded, each cysteine pair is represented by a vector containing 521 features (dimensions), combining both sequence profile and DOC information. Based on all the training vectors, a SVM is trained using LIBSVM [30]. LIBSVM is a library for support vector machines, which allows users to use different SVM implementations as a tool in their frameworks. In this work, the *C*-support vector classification (*C*-SVC) SVM was used. This formulation was designed for a given set of training vectors in two different classes [31], which matches the disulfide bond determination problem. The procedure proposed in [32] was followed to increase the classification accuracy of the SVM model trained.

The scaling of the data was not necessary, since the values of each feature $v \in [0,1]$. Next, all four possible kernel function were tested and, as expected, the radius based function (RBF) kernel produced the best results. This kernel nonlinearly maps data into a higher dimensional space being able to handle the case when the relation between class-labels (true or false disulfide bond) and attributes (vector features) is nonlinear. RBF required two parameters denoted as *C* and γ. The parameter *C* represents the penalty parameter used by the *C*-SVC SVM formulation, while the parameter γ is used in the RBF kernel function. A detailed description of the SVM formulae and other advantages of the RBF kernel are discussed in [30, 32].

The selection of both parameters *C* and γ are crucial for the success of the SVM model classification. Therefore, a grid-search was carried on *C* and γ using 5-fold cross-validation to define the best values for each parameter. The values found to optimize the results of the RBF kernel trained are: $C = 32$ and $\gamma = 0.0078125$. Lastly, the two classes studied (whether there exist a disulfide bond or not) are unbalanced as generally there are much less disulfide bonds formed in a protein than the total number of possible disulfide bonds. The problem is solved by the addition of a factor (weight) denoted as *w* used to increase the penalty parameter *C* for the pairs classified as non-disulfide bonded.

After exhaustively testing different values for *w*, the best results were found when any value in the range of $10 \leq w \leq 25$ was used.

With the SVM formulation selected, the optimal kernel chosen and all the required parameter defined and calculated, a SVM model was trained based on 439 proteins. This model is then used by the pair-wise modeling stage to calculate the probability estimate of the occurrence of a S-S bond in every cysteine pair *i* and *j* classified.

In the second (pattern-wise) modeling level, the S-S determination is tackled from a global perspective. In this scenario, the framework performs two distinct steps: (1) filters the S-S bonded pairs found in the first stage using the disulfide connectivity obtained by the MS-based framework (global information). (2) It also uses cysteine separations profiles [16] (CSPs) to find similar disulfide connectivity patterns between the different possible bonding arrangements (in analysis) and the training dataset (439 proteins). The filtering step removes all S-S bonded pairs classified in the first stage which conflict with the disulfide bonds found by the MS-based framework. This filtering is based on the fact that the predictive techniques are used to fill in the limitations of the mass spectrometry data. In fact, this filtering procedure reduced considerably the number of false positives found by the predictive framework.

Next, the method calculates the different cysteine separations profiles for the protein in analysis, considering all possible combinations of bonded pairs resulting from the filtering in the previous step. Possessing all different CSPs, the framework performs a CSP search. This search compares the CSPs calculated with the CSPs of all the proteins in the training dataset and returns the most resembled cysteine separations profile found for each CSP considered.

Match score for S-S bonds determined using predictive techniques

Each modeling stage aforementioned generates a score for each disulfide bond predicted. The SVM model used to classify disulfide bonds in the pair-wise stage calculates a probability indicating the potential of bonding for each disulfide bond classified. This probability can be further interpreted as how confident the first stage is toward the prediction. A confidence score is calculated in Eq. 5, where p_{bond} is the probability estimate for the bonding arrangement and *exp(.)* is the exponential function. This function is used to decrease the number of false positives, since it maximizes the higher p_{bond} values found, due to its exponential growth.

$$S_{SVM} = exp(p_{bond}) \qquad (5)$$

For the pattern-wise modeling stage, the score is calculated using Eq. 6 from [19], where D is the divergence between two cysteine separations profiles. The score S_{CSP} is

inversely proportional to the divergence D. When a perfect CSP match is found ($D = 0$), the score S_{CSP} is maximum ($S_{CSP} = 1$).

$$S_{CSP} = \left(1 + \log_{10}\left(1 + \frac{D}{10}\right)\right)^{-1} \qquad (6)$$

The overall match score for disulfide bonds determined using the predictive framework developed is calculated by Eq. 7.

$$V_p = S_{SVM} + S_{CSP} \qquad (7)$$

Determining the globally consistent bond topology

Once all putative S-S bonds are identified using both MS-based method and predictive techniques, they need to be integrated to obtain a globally consistent view. The approach to this problem is motivated by Fariselli and Casadio [7]. Specifically, the location of the putative disulfide bonds is modeled by edges in an undirected graph G (V, E), where the set of vertices V corresponds to the set of cysteines. To each edge, a match score (calculated in the previous sections) is assigned. The most probable disulfide connectivity is found by solving the maximum weight matching problem for the graph G. A matching M in the graph G is a set of pair-wise non-adjacent edges; that is, two edges do not share a common vertex. A maximum weight matching is defined as a matching M that contains the largest possible sum of the weights of each possible edge. For this, the

implementation of the Gabow algorithm [33] designed in [34] is used. The final protein's disulfide linkage is then converted to a user friendly graphical format in which the entire protein primary sequence is illustrated and the disulfide bonds are highlighted.

Results

The proposed method was validated utilizing experimental data obtained using a capillary liquid chromatography system coupled with either a Thermo-Fisher LCQ ion trap or a LTQ ion trap mass spectrometer LC/ESI-MS/MS system. Details of the experimental protocols can be found in [35-39]. This work used data from nine eukaryotic glycosyltransferases. These molecules and their Swiss-Prot ID are: ST8Sia IV [Q92187], Beta-lactoglobulin [P02754], FucT VII [Q11130], C2GnT-I [Q09324], Lysozyme [P00698], FT III [P21217], β1-4GalT [P08037], Aldolase [P00883], and Aspa [Q9R1T5].

Six sets of experiments were conducted to investigate the proposed method and its efficacy. These experiments included: (1) Analysis of method's efficiency, showing how the method successfully reduced the *DMS* and *FMS* search spaces. (2) Analysis of the effect of incorporating multiple ion types, demonstrating the importance of considering non-*b*/*y* ions in the determination of disulfide bonds. (3) Analysis of the effect of integrating the predictive framework with the MS-based framework, showing that the

former contributed positively to the overall method's accuracy. (4) Comparative analysis of the proposed method with established predictive techniques. (5) Comparative analysis of the method with MassMatrix, an established MS-based approach which can be used for determining S-S bonds. In both experiment 4 and experiment 5, the aforementioned set of glycosyltransferases and their known S-S bond topology provided the ground truth. (6) Analysis of the method in terms of established performance measures: *Accuracy* (Q_2), *Sensitivity* (Q_c), *Specificity* (Q_{nc}), and *Matthew's correlation coefficient (c)*.

Analysis of efficiency of the search

One of the most important characteristics of the proposed method is its efficiency in terms of excluding significant portions of a large and rapidly expanding search space. In Table 3 the size of the complete *DMS* (containing all the disulfide-bonded peptide structures generated for each protein) and the complete *FMS* (containing all the disulfide-bonded fragment ions) are compared with the truncated *DMS* and *FMS* obtained using the proposed approach.

Table 3 - *DMS* and *FMS* mass space sizes comparison

Protein	Disulfide Bond	Full Search (exponential)		Proposed Search (polynomial)		DMS decrease	FMS decrease
		DMS size	FMS size	DMS size	FMS size		
Beta-LG	$C^{82}C^{176}$	2152	2169	1870	78	13.1%	96.4%
ST8Sia IV	$C^{142}C^{292}$	1246	1792	1038	106	16.7%	94.1%
	$C^{156}C^{356}$	1246	2640	1038	255	16.7%	90.3%

FucT VII	$C^{318}C^{321}$	581	115	528	34	9.1%	70.4%
	$C^{68}C^{76}$	879	103	681	41	22.5%	60.2%
	$C^{211}C^{214}$	879	1819	681	107	22.5%	94.1%
B1,4-GalT	$C^{134}C^{176}$	2149	1189	1127	77	47.6%	93.5%
	$C^{247}C^{266}$	2149	5480	1127	426	47.6%	92.2%
Average DMS and FMS decrease						21.8%	86.4%

It may be noted that across the molecules, on an average, the proposed approach required examining about 78% of the entire *DMS* and only about 14% of the entire FMS. It is crucial to note that this reduction in search was achieved without impacting the accuracy and having considered all multiple fragment ion types (a, b, b^o, b^*, c, x, y, y^o, y^*, and z). The *DMS* decrease was less than the *FMS decrease* because the disulfide-bonded structures in the *DMS* were bigger and fewer in number and consequently dispersed across the spectra mass range. In Figure 12, the actual time taken to obtain a solution by generating the complete *DMS* and *FMS* is analyzed, as well as their truncated counterparts, for each of the molecules.

Figure 12 – Comparison of the computational time (in seconds) for the exhaustive and partial generation of *DMS* and *FMS* of the proteins from Table 3. On average there was a 49.5% decrease in time to compute the *DMS* and 88.7% decrease in time to compute the *FMS*. The computations were carried out on an Intel T2390 1.86 GHz single-core processor with 1GB RAM.

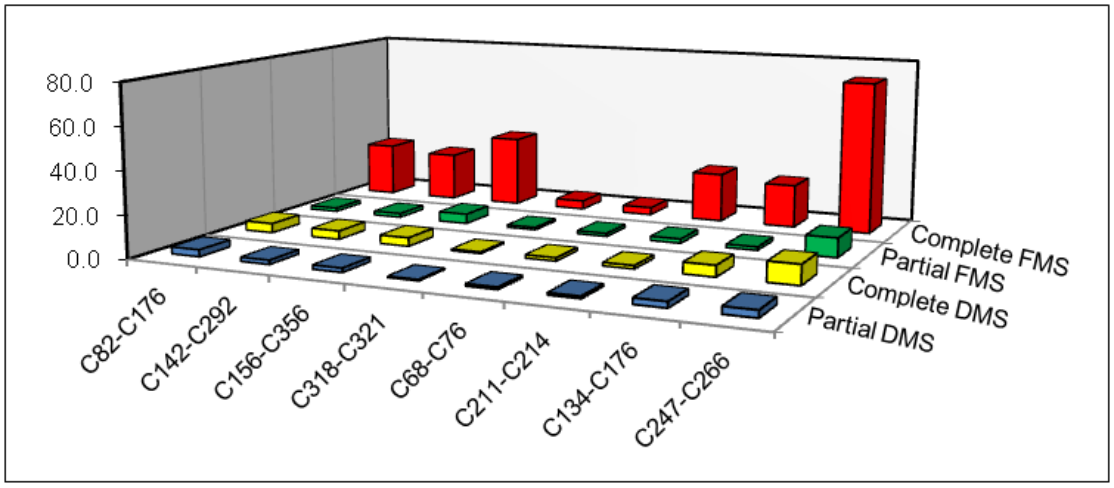

Effects of incorporating multiple ion types: A case study

In this experiment, the effect of incorporating multiple ion types (*a*, *b*, b^o, b^*, *c*, *x*, *y*, y^o, y^*, and *z*) in determining the S-S bonds as opposed to considering only *b*/*y*-ions are investigated. It was found that multiple instances of combinations between *b*/*y* ions and other ions types occurred by analyzing the confirmatory matches for the different disulfide bonds. These combinations are available in the Appendix C.

The consideration of multiple ion types also contributed to the method's accuracy in terms of determining specific S-S bonds. Disulfide bonds previously missed due to their low match score could be identified when all ten different ion types were considered. The tryptic-digested protein FucT VII (which underwent *CID*) constituted one such example. In FucT VII the bond C^{318}-C^{321} was missed when considering only *b*/*y* ions (match score 29, *pp*=11, *pp2* =15). However, as shown in Figure 13, this bond was

identified when multiple ions types were included (match score 100, *pp*=31, *pp*2=70). The confidence measures *pp* and *pp2* are described in the Comparative studies with MassMatrix section.

Figure 13 – Spectra samples from tryptic digested protein FucT VII Spectra (m/z vs. normalized intensity) illustrating the confirmatory matches (whose intensity values were at least 10% of the maximum intensity) found for the disulfide bond between cysteines C^{318}-C^{321} in protein FucT VII. The spectrum in the left shows the matches found when multiple ions were considered. The spectrum in the right shows the matches when only *b*/*y*-ions were considered.

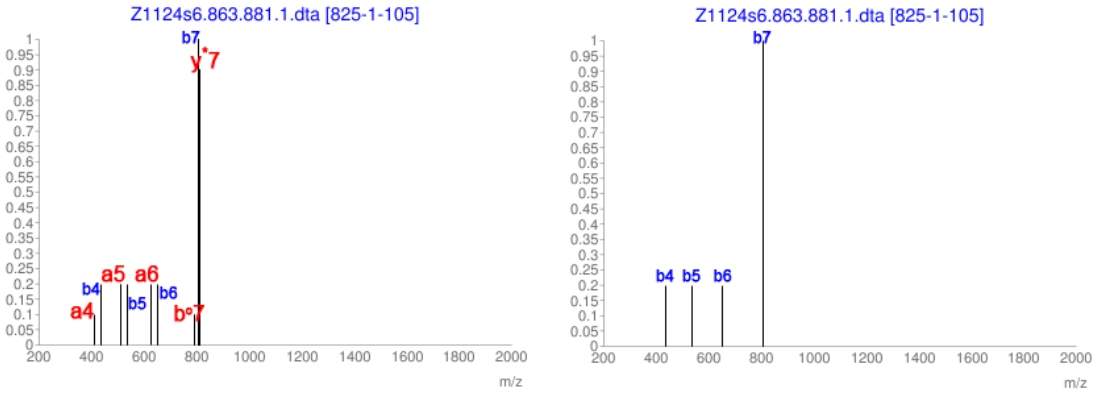

The disulfide bond C^{318}-C^{321} is used to explain this improvement. This bond is an intra-bond involving cysteines that are close together. Consequently, CID-based fragmentation was poor and the consideration of other ion types essentially improved the signal-to-background contrast. In this particular case, five other ion types - a_4, a_5, a_6, b^o_7, y^*_7 - were present in the FucT VII MS/MS data besides the *b* ions represented in the spectrum on the right in Figure 13. In the following, details of how these ions contribute to the match score V_s (from Eq. (4)) are reviewed. Two cases are presented: consideration

of only *b/y*-ions (Eq. (8)) and consideration of multiple ion types (Eq. (9)). The numerator specifies the contribution of each spectrum peak from Figure 13 (the ion corresponding to each $VM_i \times I_N$ term is showed in brackets).

$$V_S = \left(\frac{0.1784[b_4] + 0.1732[b_5] + 0.1574[b_6] + 1.4324[b_7]}{6.7321} \right) \times 100 = \left(\frac{1.9414}{6.7321} \right) \times 100 = 28.8 \qquad (8)$$

$$V_S = \left(\begin{matrix} 0.1784 \times [b_4] + 0.1732 \times [b_5] + 0.1574 \times [b_6] + 1.4324 \times [b_7] + 0.1863 \times [a_4] + \\ 0.6787 \times [a_5] + 0.1996 \times [a_6] + 0.1464 \times [b^o{}_7] + 3.5797 \times [y^*{}_7] \end{matrix} \Big/ 6.7321 \right) \times 100 \qquad (9)$$
$$= (6.7321/6.7321) \times 100 = 100.0$$

It was also observed that the consideration of multiple ion-types led to significant increase in the match scores of the true disulfide bonds, whereas only a modest increase was noticed for false positives. This allowed the increase of the threshold used on the match score V_s to identify high-quality matches from 30 to 80 (a 166% increase). The positive effect of this increment on the specificity of the method can be illustrated by considering the protein Aldolase. In this molecule, consideration of only *b*/*y* ions led to a false positive S-S bond identification between cysteines C^{135}-C^{202} (V_s=30.8, with (original) threshold 30). However, when the multiple ions-types were considered with the (increased) threshold on the match score, no S-S bond was found between C^{135}-C^{202} (V_s= 53.2, (incremented) threshold 80).

Effects of integrating the predictive framework with the MS-based framework

The integration of the predictive framework to the methodology designed and implemented allowed the identification of two disulfide bonds that were missed when only the MS-based framework was used. The combination of both state-of-the-art techniques (MS-based and predictive) allowed this work to achieve a very high accuracy, missing just one disulfide bond in 17 true positives for seven different proteins. Its specificity also became remarkable, since just one true negative S-S bond was missed. The two newly disulfide bonds predicted were: (1) an intra-bond in the Beta-LG protein which could not be found due to a blind spot caused by the same intra-bond, making the protein's fragmentation difficult. (2) One disulfide bridge in the C2GnT-I protein which could not be found since the precursor ion cannot be formed by chymotryptic digestion, which was the digestion carried for C2GnT-I.

Comparative studies with predictive techniques

In this experiment the proposed method was compared with three well known predictive methods DiANNA [12], DISULFIND [11], and PreCys [18]. The results from each of the methods are shown in Table 4 along with the with the known disulfide bond linkages according to the Swiss-Prot knowledgebase. As it can be seen, in terms of correct identifications (as well as minimizing false positives), the proposed approach outperformed all the predictive techniques.

Table 4 – Comparison with predictive methods

Protein	Known Pattern	Proposed Algorithm	DiANNA 1.1	DISULFIND	PreCys
ST8Sia IV	$C^{142}C^{292}$, $C^{156}C^{356}$,	$C^{142}C^{292}$, $C^{156}C^{356}$	$C^{11}C^{156}$,$C^{142}C^{292}$,$C^{169}C^{356}$	None	$C^{142}C^{356}$, $C^{156}C^{292}$
Beta-LG	$C^{82}C^{176}$, $C^{122}C^{135}$	$C^{82}C^{176}$, $C^{122}C^{135}$	$C^{12}C^{137}$, $C^{82}C^{176}$, $C^{126}C^{135}$	None	None
FucT VII	$C^{68}C^{76}$, $C^{211}C^{214}$, $C^{318}C^{321}$	$C^{68}C^{76}$, $C^{211}C^{214}$, $C^{318}C^{321}$	$C^{68}C^{321}$, $C^{76}C^{211}$, $C^{214}C^{318}$	$C^{76}C^{318}$	$C^{68}C^{76}$, $C^{211}C^{214}$, $C^{318}C^{321}$
B1,4-GalT	$C^{134}C^{176}$, $C^{247}C^{266}$	$C^{134}C^{176}$, $C^{247}C^{266}$	$C^{23}C^{176}$, $C^{30}C^{144}$, $C^{266}C^{341}$	None	$C^{134}C^{247}$, $C^{176}C^{266}$
C2GnT-I	$C^{59}C^{413}$, $C^{100}C^{172}$, $C^{151}C^{199}$, $C^{372}C^{381}$	$C^{59}C^{413}$, $C^{100}C^{172}$, $C^{151}C^{199}$, $C^{372}C^{381}$	$C^{13}C^{172}$, $C^{59}C^{217}$, $C^{151}C^{234}$, $C^{199}C^{372}$, $C^{381}C^{413}$	Not supported	$C^{59}C^{381}$, $C^{100}C^{372}$, $C^{151}C^{172}$, $C^{199}C^{413}$
Lysozyme	$C^{24}C^{145}$, $C^{48}C^{133}$	$C^{24}C^{145}$, $C^{48}C^{133}$,	$C^{24}C^{145}$, $C^{48}C^{133}$, $C^{82}C^{98}$, $C^{94}C^{112}$	$C^{24}C^{145}$, $C^{48}C^{133}$, $C^{82}C^{98}$, $C^{94}C^{112}$	$C^{82}C^{145}$
FT III	$C^{81}C^{338}$, $C^{91}C^{341}$	$C^{81}C^{338}$	$C^{16}C^{91}$, $C^{81}C^{143}$, $C^{129}C^{338}$	None	$C^{81}C^{91}$
Aldolase	None	None	$C^{73}C^{339}$, $C^{135}C^{290}$, $C^{115}C^{240}$, $C^{178}C^{202}$	None	None
Aspa	None	None	$C^{4}C^{275}$, $C^{60}C^{217}$, $C^{66}C^{151}$, $C^{123}C^{145}$	None	None

Comparative studies with MassMatrix

At the state-of-the-art, MS2Assign [20] and MassMatrix [24] are two MS-based methods that can be applied to the problem of determining S-S bond connectivity. In the work of Lee and Singh [3], the MS2DB system developed was found to be comparable to MS2Assign [20], albeit, in limited testing. Since the proposed method improves upon MS2DB, only detailed comparative results with MassMatrix [24] is shown in Table 5. As

part of this experiment, for each S-S bond, in addition to the empirical match score (Eq. (4)), a probability based scoring model proposed in [6] was implemented. This model provided two scores called *pp* and *pp2* scores. The *pp* score helps to evaluate whether the number of *VMs* could be a random. The *pp2* score evaluates whether the total abundance (intensity) of *VMs* could be a random. A detailed description and formulae of the *pp* and *pp2* scores is presented in [6]. The reader may note that the proposed method had better *pp* and *pp2* scores when compared to MassMatrix (higher *pp* and *pp2* scores are better, indicating smaller *p*-values). While the match scores (V_s) and (V_p) obtained with the proposed method were also higher than those obtained with MassMatrix (V^*_s), no inferences should be drawn as these scores are calculated differently in each of these methods. As can be seen from Table 5, every bond correctly determined by MassMatrix was also found by the method proposed in these studies. However, there were S-S bonds that were found by the proposed method but not by MassMatrix.

Table 5 - Comparison with MassMatrix. In brackets, (1) the scores (V_s) of each disulfide bond and the confidence scores (*pp* and *pp2* values*)* for the S-S bonds found by the MS-based framework and (2) the scores (V_p) and their components (S_{SVM} and S_{CSP}) of each disulfide bond found by the predictive framework.

Protein	Known Pattern	Proposed Method	MassMatrix
ST8Sia IV	$C^{142}C^{292}$, $C^{156}C^{356}$	$C^{142}C^{292}$ [V_s*:131;pp:109;pp2:41*], $C^{156}C^{356}$ [V_s*:100;pp:97;pp2:6*]	$C^{142}C^{292}$ [V^*_s*:54;pp:15;pp2:13*], $C^{156}C^{356}$ [V^*_s*:77;pp:23;pp2:15*]
Beta-LG	$C^{82}C^{176}$, $C^{122}C^{135}$	$C^{82}C^{176}$ [V_s*:100;pp:49;pp2:16*], $C^{122}C^{135}$ [V_p*:7.09;*S_{SVM}*:6.37;*S_{CSP}*:0.72*]	$C^{82}C^{176}$ [V^*_s*:68;pp:14;pp2:14*]
FucT VII	$C^{68}C^{76}$, $C^{211}C^{214}$,	$C^{68}C^{76}$ [V_s*:105;pp:41;pp2:98*],	$C^{68}C^{76}$ [V^*_s*:12;pp:9;pp2:3*],

	$C^{318}C^{321}$	$C^{211}C^{214}$ [V_s:100;pp:13;pp2:20], $C^{318}C^{321}$ [V_s:100;pp:31;pp2:70]	$C^{211}C^{214}$ [V^*_s:78;pp:16;pp2:11], $C^{318}C^{321}$ [V^*_s:46;pp:28;pp2:16]
B1,4-GalT	$C^{134}C^{176}$, $C^{247}C^{266}$	$C^{134}C^{176}$ [V_s:100;pp:61;pp2:29], $C^{247}C^{266}$ [V_s:195;pp:88;pp2:177]	$C^{134}C^{176}$ [V^*_s:34;pp:9;pp2:7], $C^{247}C^{266}$ [V^*_s:31;pp:7;pp2:7]
C2GnT-I	$C^{59}C^{413}$, $C^{100}C^{172}$, $C^{151}C^{199}$, $C^{372}C^{381}$	$C^{59}C^{413}$ [V_s:158;pp:237;pp2:61], $C^{100}C^{172}$ [V_p:15.03;S_{SVM}:14.48;S_{CSP}:0.55], $C^{151}C^{199}$ [V_s:100;pp:93;pp2:15], $C^{372}C^{381}$ [V_s:100; pp:81;pp2:79]	None
Lysozyme	$C^{24}C^{145}$, $C^{48}C^{133}$	$C^{24}C^{145}$ [V_s:140;pp:65;pp2:88], $C^{48}C^{133}$ [V_s:100;pp:62;pp2:55], $C^{82}C^{94}$ [V_p:10.15;S_{SVM}:9.53;S_{CSP}:0.62]	$C^{48}C^{133}$ [V^*_s:135;pp:51;pp2:33]
FT III	$C^{81}C^{338}$, $C^{91}C^{341}$	$C^{81}C^{338}$ [V_s:100;pp:179;pp2:93]	None
Aldolase	None	None	None
Aspa	None	None	None

Quantitative assessment and analysis of the method's performance

If the set of disulfide bonds are denoted by *P* and the set of cysteines not forming disulfide bonds by *N*, then true positive (*TP*) predictions occur when disulfide bonds that exist are correctly predicted. False negative (*FN*) predictions occur when bonds that exist are not predicted as such. Similarly, a true negative (*TN*) prediction correctly identifies cysteine pairs that do not form a bond. Finally, a false positive (*FP*) prediction, incorrectly assigns a disulfide link to a pair of cysteines, which are not actually bonded. Based on these definitions, the following four standard measures were used to analyze the proposed method.

$$\text{Sensitivity } (Q_c) = TP/P \qquad (10)$$

$$\text{Specificity } (Q_{nc}) = TN/N \qquad (11)$$

$$\text{Accuracy } (Q_2) = TP + TN/P + N \qquad (12)$$

$$\text{Matthew's correlation coefficient (c)} = \frac{TP \times TN - FP \times FN}{\sqrt{(TP + FN)(TP + FP)(TN + FP)(TN + FN)}} \qquad (13)$$

Table 6 presents the results obtained for the method developed. With maximum specificity and high accuracy (99% average), the method correctly reported the connectivity for most of the proteins. The method only failed to identify one cross-linked bond in the FT III protein because this particular connectivity configuration creates a large disulfide-bonded structure, which is poorly fragmented by tandem mass spectrometry. It was also not identified by the predictive framework. It is important to note that neither MassMatrix nor MS2Assign were able to this disulfide bridge.

Table 6 - Sensitivity, specificity, accuracy and Mathew's correlation coefficient results for all nine proteins analyzed.

Protein	Q_c	Q_{nc}	Q_2	c
ST8Sia IV	1.00	1.00	1.00	1.00
Beta-LG	1.00	1.00	1.00	1.00
FucT VII	1.00	1.00	1.00	1.00
C2GnT-I	1.00	1.00	1.00	1.00
Lysozyme	1.00	0.96	0.96	0.80
B1,4-GalT	1.00	1.00	1.00	1.00
FT III	0.50	1.00	0.94	0.69
Aldolase	X	1.00	1.00	X
Aspa	X	1.00	1.00	X

Software

The integration of both state-of-the-art MS-based and predictive frameworks was consolidated in the newly released application MS2DB+. MS2DB+ is a platform-independent web application that efficiently determines the disulfide linkage in proteins based on mass spectrometry data and machine learning techniques. The software can account for multiple ions (*a*, *b*, b^o, b^*, *c*, *x*, *y*, y^o, y^*, and *z*) in determining the disulfide bonds. It also uses a SVM-based model and cysteine separations profiles to increase the disulfide connectivity prediction accuracy. MS2DB+ is publicly available at: http://tintin.sfsu.edu/~whemurad/disulfidebond/. Its source code is accessible at http://code.google.com/p/disulfidebond/ under the Apache License 2.0.

Implementation

MS2DB+ was coded in PHP and currently runs on an Apache web server. PHP is a widely-used general-purpose scripting language that is especially suited for web development. Apache is the most popular HTTP server available, becoming the first web server software to surpass the 100 million web site milestone, according to a web server survey conducted by Netcraft in 2009. In MS2DB+, the disulfide bond determination can be done in two modes: standard analysis (completely automatic) and advanced analysis (user may customize thresholds and parameters).

Both of these modes require three inputs: (a) a ZIP file containing any of the standard file formats used to store mass spectrometry data (i.e. mzXML, mzML, mzData or *Sequest* DTA files), (b) the protein sequence in FASTA format and (c) the protease used to digest the protein sample. Other non-standard file formats generated by different tandem MS/MS methods can be converted to one of the acceptable file formats using the open-source framework ProteomeCommons.org IO, created by Jayson Falkner and freely available at (www.proteomecommons.org/current/531/).

XML-based file formats became the standard open-source data formats for storage and exchange of mass spectrometry data. The Extensible Markup Language (XML) aids to the simplicity, generality and usability of the data. It allows research groups from all over the world to use the same set of rules for encoding MS information, opening the possibility of a common file format for MS data exchange worldwide.

Initially developed by the SPC/Institute for Systems Biology, mzXML is one of the most common formats of mass spectrometry data exchange. It provides a container for MS and MS/MS proteomics data. Another significant advantage is the fact that most of the raw, proprietary file formats from most mass spectrometer vendors can be converted to the open mzXML format. mzData was developed by the Human Proteome Organization (HUPO) and offers similar functionalities to mzXML. mzML is the mass spectrometry data format developed by the Mass Spectrometry Standards Working Group

of the HUPO Proteomic Standards Initiative (HUPO-PSI). mzML is the combined effort of research centers and instrument vendors worldwide to replace the currently most used mzXML and mzData formats by a single XML-based format.

The utilization of the predictive framework in the determination of disulfide connectivity can be easily triggered in both modes. This novel and powerful integration is activated by a single user click. Users can choose whether or not to include predictive techniques in the analysis of S-S linkage. If both frameworks are turned on, the application distinguishes the disulfide bonds found by showing the different match scores V_s and V_p for each bond, as well as a note depicting the S-S bridges found by the SVM-based predictive framework.

The key parameters users can customize include: initial and confirmatory matching thresholds, MS/MS intensity/abundance threshold which contributes to suppressing MS-data noise, and the trimming parameters ε and δ, which are used to trim the theoretical spectra during the *Initial* and *Confirmatory Matching* stages respectively. Optionally, in both interfaces, the user may also (a) choose different combinations of multiple ion types to be considered during the spectral matching (based on knowledge of the dissociation method); (b) select the number of missing cleavage sites during protein's digestion; and (c) specify the protein region where a disulfide bond is not expected to occur.

Usage Example

Here, a walkthrough demonstrating the use of MS2DB+ using the protein Syalyltransferase ST8Sia IV (UniProt ID Q92187) is described. This example is one of nine Glycosyltransferases with varying S-S bonding topologies, the MS/MS data for which have been made available in the *Datasets* page of the MS2DB+ site.

As a first step, in the standard analysis page (Fig.14.A), the user needs to upload a ZIP file containing the corresponding set of data file(s), enter the protein's FASTA sequence and select the protease used during digestion. Next, MS2DB+ analyzes the data and lists the disulfide bonds found with either (1) their empirical and statistical scores calculated for S-S bonds found by the MS-based framework or (2) their empirical scores S_{SVM} and S_{CSP} combined for the disulfide bridges found by the SVM-based framework. Each bond is shown graphically, as in Fig.14.B where two bonds (C^{142}-C^{292} and C^{156}-C^{356}) are shown. MS2DB+ also provides other relevant information for each disulfide bond found by the MS-based framework, including (1) the disulfide-bonded peptide structure and the data file involved in the initial match, (2) a graph containing the most abundant spectral matches (Fig.14.D), (3) the list of confirmatory matches along with the fragment ions matched (theoretical and experimental), (4) their respective mass values and mass difference (both measured in Daltons), and (5) the fragments charge state (z) and the peaks normalized intensity (abundance) (Fig.14.C). Each confirmatory match

whose normalized intensity (abundance) is found to be equal or greater than 50% is highlighted in green to facilitate rapid identification.

Figure 14 - (A) The standard analysis interface of MS2DB+ showing the key inputs for the molecule ST8SiaIV. (B) Disulfide bonds (in yellow) found for ST8SiaIV. (C) Some of the confirmatory matches found for the S-S bond between cysteines C^{142}-C^{292}. Matches whose MS/MS fragment's normalized intensity equal or exceed 50% are marked in green). (D) The confirmatory spectrum for an initial match (in red) containing the most abundant confirmatory peaks found while determining the S-S bond between cysteines C^{142}-C^{292}.

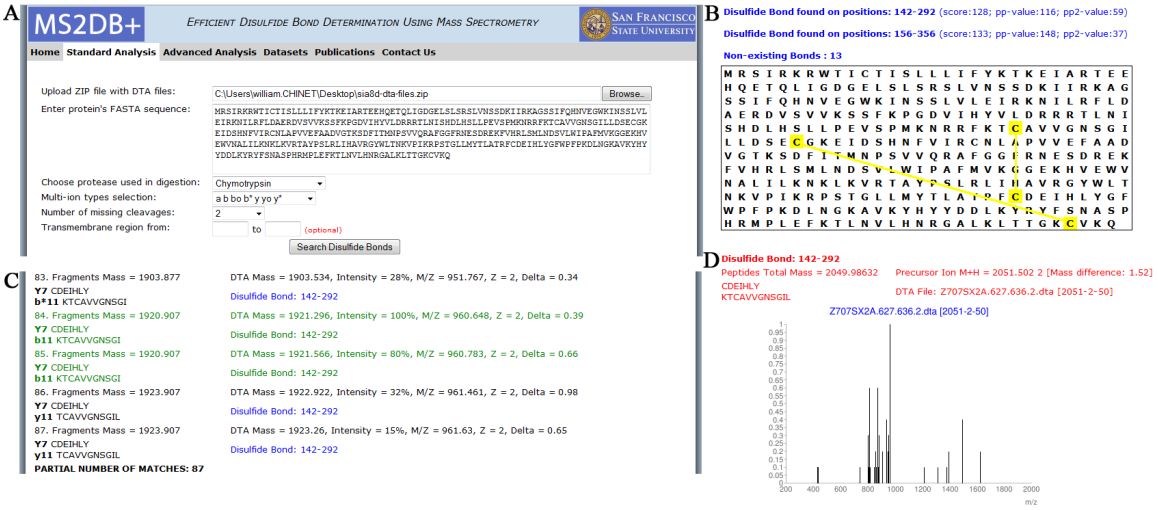

Conclusions

An algorithmic methodology combining a MS-based framework and a predictive SVM-based framework was presented for determining S-S bond topologies of molecules. The method uses MS/MS data and machine learning techniques based on pair-wise and pattern-wise disulfide linkage information. The proposed approach is computationally

efficient, data driven, and has high accuracy, sensitivity, and specificity. It is not limited either by the connectivity pattern or by the variability of product ion types generated during the fragmentation of precursor ions. Furthermore, the approach does not require user intervention and can form the basis for high-throughput S-S bond determination. The complete method developed here was fully implemented and is publicly available at http://tintin.sfsu.edu/~whemurad/disulfidebond. The web application created is called MS2DB+.

References

1. Singh R: **A review of algorithmic techniques for disulfide-bond determination**. *Briefings in Functional Genomics and Proteomics,* 2008, 7(2), pp. 157-172.
2. Nesvizhskii AI, Vitek O, Aebersold R: **Analysis and validation of proteomic data generated by tandem mass spectrometry**. *Nature Methods,* 2007, 4(10), pp. 787-797.
3. Lee T, Singh R: **Comparative Analysis of Disulfide Bond Determination Using Computational-Predictive Methods and Mass Spectrometry-Based Algorithmic Approach**. *BIRD*, CCIS 13, 2008, pp. 140-153.
4. Johnson RS, Martin SA, Biemann K, Stults JT, Watson JT: **Novel fragmentation process of peptides by collision-induced decomposition in a tandem mass**

spectrometer: differentiation of leucine and isoleucine. *Anal Chem*, 1987, 59:2621

5. Steen H, Mann M: **The abc's (and xyz's) of peptide sequencing**. *Nature Reviews, Molecular Cell Biology*, 5, 2004, pp.699-711
6. Xu H, Freitas MA: **A mass accuracy sensitive probability based scoring algorithm for database searching of tandem mass spectrometry data**. *BMC Bionformatics 2007*, 8:133-142
7. Fariselli P, Casadio R: **Prediction of disulfide connectivity in proteins**. *Bioinformatics* 2001, 17, 957-64.
8. Fariselli P, Riccobelli P, Casadio R, **Role of evolutionary information in predicting the disulfide-bonding state of cysteines in proteins**, Proteins, 36, 1999, 340-346
9. Fariselli P, Martelli PL, Casadio R, **A neural network base method for predicting the disulfide connectivity in proteins**, Knowledge based Intelligent Information Engineering Systems and Allied Technologies KES, 2002, Vol. 1, IOS Press, p 464-468
10. Vullo A, Frasconi P, **Disulfide connectivity prediction using recursive neural networks and evolutionary information**, BIOINFORMATICS, Vol. 20 no. 5 2004, pages 653–659 DOI: 10.1093/bioinformatics/btg463

11. Ceroni A et al: **DISULFIND: A Disulfide Bonding State and Cysteine Connectivity Prediction Server**. *Nucleic Acids Research* 2006; 34:177-181.
12. Ferre F, Clote P: **DiANNA: A Web Server for Disulfide Connectivity Prediction**. *Nucleic Acids Research* 2005; 33:230-232.
13. Ferre F, Clote P, **Disulfide Connectivity prediction using secondary structure information and diresidue frequencies**, Bioinformatics, Vol. 21, No. 10, 2005, 2336-2346, doi:10.1093/bioinformatics/bti328
14. Altschul SF, et al, **Gapped BLAST and PSI-BLAST: a new generation of protein database search programs**, Nucleic Acid Research, 1997, Vol. 25, No. 17, 3389-3402
15. Jones DT, **Protein secondary structure prediction based on position-specific scoring matrices**, J. Mol Biol. 292195-202, 1999
16. Zhao E, et al, **Cysteine separations profiles on protein sequences infer disulfide connectivity**, BIOINFORMATICS, Vol. 21 no. 8 2005, pages 1415–1420 doi:10.1093/bioinformatics/bti179
17. Chen YC, Hwang JK, **Prediction of Disulfide Connectivity from Protein Sequences**, PROTEINS: Structure, Function, and Bioinformatics 61, 2005, 507-512
18. Tsai CH et al: **Improving disulfide connectivity prediction with sequential distance between oxidized cysteines**. *Bioinformatics* 2005, 21:4416-4419

19. Chen BJ, Tsai CH, Chan CH, Kao CY, **Disulfide Connectivity Prediction with 70% Accuracy Using Two-Level Models**, PROTEINS: Structure, Function, and Bioinformatics 64:246–252, 2006

20. Schilling B et al: **MS2Assign, automated assignment and nomenclature of tandem mass spectra of chemically crosslinked peptides**. *J Am Soc Mass Spectrom.*, 14(8):834-50, 2003

21. Yu ET, et al.: **The Collaboratory for MS3D: A New Cyberinfrastructure for the Structural Elucidation of Biological Macromolecules and Their Assemblies Using Mass Spectrometry-Based Approaches**. *J Proteome Res.* (2008). ASAP article, 10.1021/pr800443f

22. Lee T, Singh R, Yen TY, Macher B: **An Algorithmic approach to Automated High-Throughput Identification of Disulfide Connectivity in Proteins Using Tandem Mass Spectrometry**. *Proc. Computational Systems Bioinformatics, CSB*, 2007, pp. 41-51

23. Lee T, Singh R, Yen R, Macher B: **A mass-based hashing algorithm for the identification of disulfide linkage patterns in protein utilizing mass spectrometry data**. *Proc. IEEE International Symposium on Computer-Based Medical Systems, CBMS*, 2007, pp. 397-402

24. Xu H, Zhang L, Freitas MA: **Identification and Characterization of Disulfide Bonds in Proteins and Peptides from Tandem MS Data by Use of the**

MassMatrix MS/MS Search Engine. *Journal of Proteome Research*, 7, 13-144, 2008.

25. Bairoch A, Apweiler R, **The SWISS-PROT protein sequence database and its supplement TrEMBL in 2000**, Nucleid Acid Research, 2000, Vol. 28, No. 1, 45-48
26. American Society for Mass Spectrometry [http://www.asms.org]
27. Cormen TH, Leiserson CE, Rivest RL, Stein C: Introduction to Algorithms, 2nd edition, MIT Press, Cambridge, MA, U.S.A, 2001
28. Han J, Kamber M: Data Mining – Concepts and Techniques, 2nd edition, Morgan Kaufmann Publishers, San Francisco, CA, U.S.A, 2006
29. Harrison PM, Sternberg MJE, **Analysis and classification of disulphide connectivity in proteins**, J Mol Biol, 39: 4207-4216, 1994
30. Chang CC, Lin CJ, **LIBSVM: a library for support vector machines**, 2001
31. Vapnik V, **The nature of statistical learning theory**, New York, Springer, 1995
32. Hsu CW, Chang CC, Lin CJ, **A Practical Guide to Support Vector Machine**, 2003
33. Gabow HN: **An efficient implementation of Edmonds' Algorithm for Maximum Matching on Graphs**. *Journal of the ACM*, 23, 2006, 221-234
34. Rothberg E, **MATHPROG: Solver for the maximum weight matching problem** [http://elib.zib.de/pub/Packages/mathprog/matching/weighted/]

35. Thomas S, Yen TY, Macher BA: **Eukaryotic glycosyltransferases: cysteines and disulfides**. *Glycobiology*, 12, 2002, pp. 4G-7G

36. Yen TY, Macher BA: **Determination of glycosylation sites and disulfide bond structures using LC/ESI-MS/MS analysis**. *Methods in enzymology* 2006; 415:103-113

37. Angata K, Yen TY, El-Battari A, Macher B, Fukuda M, **Unique Disulfide Bond Structures Found in ST8Sia IV Polysialyltransferase Are Required for Its Activity**, *The Journal of Biological Chemistry*, VOL. 276, No. 18, May 4, 2001, pp. 15369-15377

38. Yen TY, Macher BA, Bryson S. et al, **Highly Conserved Cysteines of Mouse Core 2 β1,6-N-Acetylglucosaminyltransferase I Form a Network of Disulfide Bonds and Include a Thiol That Affects Enzyme Activity**, J Biology Chemistry, Vol. 278, No. 46, Issue 14, 45864-45881, 2003

39. Thomas S, Yen TY, Macher BA, **Eukaryotic glycosyltransferases: cysteines and disulfides**, Glyco-Forum Section, 2001

40. Murad W, Singh R, Yen TY, **An efficient algorithmic approach for mass spectrometry-based disulfide connectivity determination using multi-ion analysis**, BMC Bioinformatics, 2010

41. Murad W, Singh R, Yen TY: **Polynomial-Time Disulfide Bond Determination Using Mass Spectrometry Data**. *Proc. IEEE Computational Structural Bioinformatics Workshop, CSBW*, 2009, 79-86

42. Chen T, Jaffe JD, Church GM: **Algorithms for Identifying Protein Cross-links via Tandem Mass Spectrometry**. *Proc. RECOMB*, 2001, pp. 95-102

43. Frank A, Tanner S, Pevzner P: **Peptide Sequence Tags for Fast Database Search in Mass-Spectrometry**. *Proc. RECOMB* 2005, LNBI 3500, pp. 326-341, 2005

44. Keller A, Nesvizhskii AI, Kolker E, Aebersold R: **Empirical statistical model to estimate the accuracy of peptide identification made by MS/MS database search**. *Analytical Chemistry*, 74(20), 2002

45. Mackenzie HA, Ralston GB, Shaw DC, **Location of sulfhydryl and disulfide groups in bovine beta-lactoglobulins and effects of urea**, *Biochemistry* VOL. 11, November, 1972, pp. 4539-4547

46. de Vries T, et al, **Neighboring cysteine residues in human fucosyltransferase VII are engaged in disulfide bridges, forming small loop structures**, *Glycobiology*, VOL. 11, No. 5, December 12, 2000, pp. 423-432

47. Baldi P, Cheng J, Vullo A, **Large-scale prediction of disulphide bond connectivity**, Advances in Neural Information Processing Systems 17. Cambridge, MA: MIT Press, 2005, p 97-104

48. Platt J, **Probabilistic outputs for support vector machines and comparison to regularized likelihood methods**, Advances in Large Margin Classifiers, Cambridge, MA: MIT Press, 2000

49. Chen YC, Lin YS, Lin CJ, Hwang JK, **Prediction of the bonding states of cysteines using the support vector machines based on multiple feature vectors and cysteine state sequences**, Proteins, 55, 2004, 1036-1042

50. Fiser A, Simon I, **Predicting the oxidation state of cysteines by multiple sequence alignment**, Bioninformatics, 16, 2000, 251-256

51. Martelli PL, Fariselli P, Malaguti L, Casadio R, **Prediction of the disulfide-bonding state of cysteines in proteins at 88% accuracy**, Protein Sci., 11, 2002, 2735-2739

52. Lu CH, Chen YC, Yu CS, Hwang JK, **Predicting Disulfide Connectivity Patterns**, PROTEINS: Structure, Function, and Bioinformatics, 67, 2007, 262-270

53. Ward JJ, McGuffin LJ, Buxton BF, Jones DT, **Secondary structure prediction with support vector machines**, Bioinformatics, 19, 2003, 1650-1655

54. Abkevich VI, Shakhnovich EI, **What can disulfide bonds tell us about protein energetics, function and folding?: simulations and bioinformatics analysis**, J Mol Biol, 300, 2000, 975-985

55. Wedemeyer WJ, Welker E, Narayan M, Scheraga HA,**Disulfide bonds and protein folding**, Biochemistry, 39, 2000, 4207-4216

56. Chuang CC, et al, **Relationship between protein structures and disulfide-bonding patterns**, Proteins, 53, 2003, 1-5

57. Frasconi P, Passerini A, Vullo P, **A Two-Stage SVM Architecture for Predicting the Disulfide Bonding State of Cysteines**, Proc. of the IEEE Workshop in Neural Networks for Signal Processing, 2002, 25-34

58. Cheng J, Saigo H, Baldi P, **Large-scale prediction of disulphide bridges using kernel methods, two-dimensional recursive neural networks, and weighted graph matching**, Proteins, 62, 2006, 617-629

59. Lenffer J, Lai P, Mejaber WE, et al, **CysView: Protein Classification Based on Cysteine Pairing Patterns**, Nucleic Acid Research, 32, 2004, 350-354

60. Hogg PJ, **Disulfide bonds as switches for protein function**, Trends Biochem Sci, 28, 2003, 210-214

61. Matsumura M, Signor G, Matthews BW, **Substantial increase in proteins stability by multiple disulfide bonds**, Nature, 342, 1989, 291-293

62. Craig R, Krokhin O, Wilkins J, et al, **Implementation of an algorithm for modeling disulfide bond patterns using mass spectrometry**, J Proteome Res, 2, 2003, 657-661

63. Bafna V, Reinert K, **Mass spectrometry and computational proteomics**, Encyclopedia of Genetics, Genomics, Proteomics, and Bioinformatics. John Wiley & Sons, 2005

64. Gorman JJ, Wallis T, Pitt JJ, **Protein disulfide bond determination by mass spectrometry**, Mass Spectrom Rev, 21, 2002, 183-216

65. Morris HR, Pucci P, **A new method for rapid assignment of S-S bridges in proteins**, Biochem Biophys Res Commun, 126, 1985, 1122-1128

66. Fenyo D, **A software tool for the analysis of mass spectrometric disulfide mapping experiments**, Bioinformatics, 13, 1997, 17-18

67. Fenyo D, Beavis RC, **A Method for Assessing the Statistical Significance of Mass Spectrometry-Based protein Identifications Using General Scoring Schemes**, Anal Chem, 75, 2003, 768-774

68. McAfee KJ, Duncan DT, Assink M, Link AJ, **Analyzing Proteomes and Protein Function Using Graphical Comparative Analysis of Tandem Mass Spectrometry Results**, Molecular & Celular Proteomics, 2006, 1497-1513

69. Wu Z, Lajoie G, Ma B, **MSDASH: Mass Spectrometry Database and Search**, CSB, 2008, 63-71

70. Meija J, **Mathematical tool in analytical mass spectrometry**, Anal Bioanal Chem, 385, 2006, 486-499

71. Mormann M, Eble J, et al, **Fragmentation of intra-peptide and inter-peptide disulfide bonds of proteolytic peptides by nanoESI collision-induced dissociation**, Anal Bioanal Chem, 392, 2008, 831-838

72. Choi S, Jeong J, Na S, Lee HS, et al, **New Algorithm for the Identification of Intact Disulfide Linkages Based on Fragmentation Characteristics in Tandem Mass Spectra**, Journal of Proteome Research, 9, 2010, 626-635

Appendix A

Action of APPROX-DMS on the protein Beta-LG

An example illustrating the action of APPROX-DMS on the Beta-LG protein is shown below. Table 7 presents snapshots of the *DMS*, *TrimSet*, and *IM* sets for each CCP_i (cysteine-containing peptide) mass value, during each iteration of the trimming process.

Table 7 - DMS, TrimSet and IM mass sets for each CCPi mass value generated from the tryptic digestion of the protein Beta-lactoglobulin (Beta-LG). The values presented here are retrieved at the end of each loop cycle (lines 5-13) in Figure 4.

i	CCP_i	DMS	TrimSet	IM
0	1064	{0,1064}	{}	{}
1	1192	{0,1064, 1192, 2254}	{}	{}
2	1658	{0, 1064, 1192, 1658, 2254, 2720, 2849}	{}	{}
3	1746	{0, 1064, 1192, 1658, 1746, 2254, 2720, 2849, 2937}	{2809}	{}
4	2275	{0, 1064, 1192, 1658, 1746, 2275, 2720, 2849, 2937}	{2254, 2809}	{}
5	2477	{0, 1064, 1192, 1658, 1746, 2275, 2477, 2720, 2849,	{2254, 2809}	{}

		2937}		
6	2535	{0, 1064, 1192, 1658, 1746, 2275, 2535, 2720, 2849, 2937}	{2254, 2477, 2809}	{}
7	2648	{0, 1064, 1192, 1658, 1746, 2275, 2535, 2648, 2720, 2849, 2937}	{2254, 2477, 2809}	{}
8	2776	{0, 1064, 1192, 1658, 1746, 2275, 2535, 2648, 2776, 2849, 2937}	{2254, 2477, 2720, 2809}	{}
9	2790	{0, 1064, 1192, 1658, 1746, 2275, 2535, 2648, 2776, 2849, 2937}	{2254, 2477, 2720, 2790, 2809}	{}
10	2930	{0, 1064, 1192, 1658, 1746, 2275, 2535, 2648, 2776, 2849, 2937}	{2254, 2477, 2720, 2790, 2809, 2930}	{}
11	3189	{0, 1064, 1192, 1658, 1746, 2275, 2535, 2648, 2776, 2849, 2937, 3189}	{2254, 2477, 2720, 2790, 2809, 2930}	{3189}

Appendix B

Etudes of the proof of polynomial complexity

The proof that the proposed method is a fully polynomial approximation scheme consists of two parts. First, we need to show that each value returned by the APPROX-DMS function is within $1+\varepsilon$ from the optimal solution. Second, we need to show that the running time of the method is fully polynomial. We refer the reader to [27] for the proof of the first part and focus in the following on analyzing the complexity of the method. To show that the method is a fully polynomial-time approximation scheme, we derive a bound on the length of a DMS set. After trimming, successive elements DMS_i and $DMS_i^{'}$ of DMS must have a relationship $DMS_i^{'}/DMS_i > 1+\varepsilon$. Therefore, each

possible DMS set contains up to $\log_{1+\varepsilon} PML_{val}$ values. Since $(x/(1+x)) \le \ln(1+x) \le x$ and $0 < \varepsilon < 1$, it can be shown that:

$$\log_{1+\varepsilon} PML_{val} = \frac{\ln PMS_{val}}{\ln 1+\varepsilon} \le \frac{(1+\varepsilon)\times \ln PMS_{val}}{\varepsilon} \le \frac{2\times \ln PMS_{val}}{\varepsilon} \qquad (11)$$

As can be seen from Eq. (11), this bound is (explicitly) polynomial in the size of the input PMS_{val}. It is also (implicitly) polynomial in the size of the set DMS since ε is directly proportional to the number of cysteine-containing peptides *k* (per Eq. (2)) and these peptides are in turn combined to form each element of the DMS. A similar argument can be made for the APPROX-FMS routine, completing thereby the proof that the proposed method is a fully polynomial-time approximation scheme.

Appendix C

Combination between b/y ions and other ions types on MS/MS data

In the following, we show that combinations between ion types other than just *b* and/or *y* ions do occur, even for proteins that underwent *CID*. Most importantly, many of these combinations were present with high abundance across the proteins we analyzed.

Table 8 - Different combinations of multiple ion types present in some of the proteins we used to validate the method proposed. For each protein, we present all combinations involving ion types other than just b and/or y ions, whose normalized

intensity (or abundance) was found to be at least 50% of the highest intensity value measured.

Protein	Disulfide Bonds	Confirmatory matches (each match is presented as a [ion types; abundance measured] pair)
ST8Sia IV	$C^{142}C^{292}$	[$b^{*}_{3}b^{o}_{5}$; 56%], [$b^{*}_{3}a_{7}$; 100%], [$c_{4}b^{o}_{5}$; 80%], [$b_{5}y^{o}_{12}$; 62%]
	$C^{156}C^{356}$	[$z_{7}b^{*}_{5}$; 66%], [$a_{8}b^{*}_{4}$; 75%], [$a_{8}a_{4}$; 69%], [$y_{4}a_{10}$; 63%]
Beta-LG	$C^{82}C^{176}$	[a_{10}; 68%], [c_{11}; 51%], [$x_{5}y^{*}_{6}$; 58%], [$x_{5}y_{14}$; 100%], [$b_{6}c_{13}$; 68%], [$c_{8}y^{*}_{14}$; 66%]
FucT VII	$C^{68}C^{76}$	[y^{*}_{7}; 57%], [$a_{5}a_{15}$; 100%], [$b^{*}_{7}b^{*}_{14}$; 57%]
	$C^{211}C^{214}$	[b^{o}_{9}; 75%]
	$C^{318}C^{321}$	[z_{7}; 100%], [y^{*}_{7}; 95%]
B1,4-GalT	$C^{134}C^{176}$	[a_{18}; 63%], [$b^{*}_{7}a_{18}$; 76%]
	$C^{247}C^{266}$	[$c_{5}c_{24}$; 100%]
C2GnT-I	$C^{59}C^{413}$	[b^{*}_{14}; 100%], [$x_{7}y^{*}_{7}$; 84%], [$z_{3}y^{o}_{11}$; 56%], [$z_{3}y^{*}_{11}$; 79%], [a_{16}; 77%], [$z_{6}c_{16}$; 77%], [$y_{9}c_{18}$; 93%], [$x_{16}y_{13}$; 79%]
	$C^{372}C^{381}$	[$c_{6}x_{8}$; 100%], [x_{23}; 52%], [$c_{9}a_{20}$; 100%], [$c_{6}b^{o}_{22}$; 98%], [$c_{6}b^{*}_{22}$; 50%]
	$C^{151}C^{199}$	[a_{9}; 100%], [$a_{3}c_{9}$; 51%], [$b^{*}_{7}b^{o}_{10}$; 72%], [$b^{*}_{7}y_{9}$; 100%], [$a_{3}b^{*}_{14}$; 65%], [$b^{*}_{4}a_{14}$; 78%]
Lysozyme	$C^{24}C^{145}$	[$x_{3}a_{6}$; 100%]
	$C^{48}C^{133}$	[$x_{2}y^{o}_{4}$; 100%], [a_{11}; 50%]